Measuring Non-Contact Respiration Rate of a Premature Infant with a Thermal Camera

Klein Meuleman, Evelien

Award date:
2019

Bachelor End Project

Measuring Non-Contact Respiration Rate of a Premature Infant with a Thermal Camera

Applied Physics

Date: 6th of November 2019
Author: Evelien Klein Meuleman
Supervisors: dr.ir. Carola van Pul (associate professor)
ir. Ilde Lorato (PhD-student)

Abstract

Research is being conducted to develop contactless monitoring of respiration of premature infants with thermography. The respiration of an infant can be determined from the temperature change of the nostrils during inhalation and exhalation or by monitoring the movement of the thorax. The goal of this work is to find the best position for a thermal camera aiming at monitoring the thorax movement of an infant. A simulator was developed to simulate the thorax motion of an infant. To investigate the influence of the camera position on the quality and robustness on the measurements different settings and positions were varied. The used method automatically selects the region of interest by selecting the pixels that display periodic behavior in the expected frequency range of breathing. The respiration rate was determined for all different settings and positions. The designed setup works and can simulate breathing, though there are limitations to the simulator as it deviates from real neonatal breathing. Further development could be an improvement of the designed setup to simulate better neonatal breathing.

Index

1. Introduction

Premature infant is an infant born before 37 weeks of gestation. Some are born so early that they are not able to survive without intensive care. A newborn premature infant is placed after birth in an incubator. An incubator ensures the correct temperature and humidity. The premature infant will be continuously monitored for vital signs, like heart rate, breathing rate, blood pressure or body temperature [2]. Many premature infants have breathing problems, because their lungs are not yet well developed. Therefore, it is important to monitor the respiration rate to check the infants' breathing pattern. Some infants are helped with breathing through a ventilator.

Currently the respiration rate of an infant is measured by using the same electrodes for measuring the electrocardiography (ECG) of the infant. During respiration alterations in electrical impedance across the chest can be measured by impedance monitoring. But this technique has some disadvantages. If the airway is obstructed, the air can still move back and forth within the chest wall cavity, making it seems like the infant is breathing. Another problem is that the signal from the heartbeat can provide a small signal making it appear that the infant is breathing, while the infant does not breathe. This is called the cardiac artifact. Moreover, the signal for the respiration rate of the infant can be disturbed by motion artifacts [14]. The respiratory rate could be measured separately to get a better signal, but the attachment of the sensors to the infants' body, induces stress and discomfort. Also, placement and removal of adhesive electrodes on premature infants frequently lead to epidermal stripping and skin disruption [13].

Therefore, research is being conducted for contactless monitoring of respiration. New monitoring solutions are based on Doppler radar and imaging sensors using visible, mid-wave infrared and long-wave infrared light [5]. Recently thermography is rediscovered for contactless monitoring of respiration in neonatal medicine. Thermography uses a thermal camera that measures the radiation energy emitted from any object containing solid matter [8]. The respiration rate of an infant can be determined in two ways with this technique. The first method is to point the thermal camera to the infant's face and measure the temperature change by the nostrils. The temperature of the nostrils will decrease by inhalation and will increase during exhalation, because the environment temperature is lower than the body temperature and the inhaled air is colder than the air that is exhaled [3]. The second method measures the movement of the thorax of the infant. When the infant inhales, the belly will expand and if the infant exhales, the belly will retract. As a result, the pixels around the thorax will change in temperature. The pixels around the thorax will vary with the same frequency as the respiration rate. Though several studies have shown its potential, more research is needed to cope with the following challenges. The first one is the movement of the infant. If the infant turns or moves, the thermal camera loses the signal of the nostrils or the belly. Likewise, the position of the infant influences the accuracy of the respiration rate signals. The position of the camera is also very important. Moreover, the respiration rate of an infant is more difficult to measure if the infant wears a ventilation mask. Furthermore, the thermal cameras are expensive and since probably several cameras are needed per baby in an incubator, this quickly becomes very expensive and very bulky.

The goal is to build a test setup to measure simulated respiration rate due to the motion of the thorax.

The format of this report is as follows: in section 2 the background is discussed. The measuring method and experimental setup are explained in section 3. The results are presented in section 4 and the discussion of the results are discussed in section 5. Finally, in section 6 the conclusion, recommendations and the future perspectives are given.

2. Background

2.1 Respiration

Figure 2.1: A photo taken at the NICU in the maxima medical center (MMC) in Veldhoven [6].

Normally, a baby is born after 40 weeks of pregnancy. Some infants are born before 37 weeks of pregnancy and, if born very premature they may have undeveloped lungs, digestive tract, immune system and skin. These infants are called premature infants. Infants born before 34 weeks of pregnancy often have circulatory problems, cerebral bleeding and serious infections, and have a lower chance of survival. Since premature infants cannot keep their temperature stable, they are placed in an incubator on the Neonatal Intensive Care Unit (NICU) [9]. Premature infants in the NICU are cared for 24 hours per day by a team of doctors, nurses and other medical professionals [11]. Neonates need continuous monitoring to check if they develop well. Examples of the vital sign that are monitored are the infant's respiration rate, oxygen saturation and heart rate. In figure 2.1 a picture of a NICU can be seen. In this picture two nurses, dressed in blue, and two parents can be seen. The parents are caring for the twins. The twins lie in separate incubators. Premature infants get stressed from sound, light, touching, temperature changes and movement.

In the first weeks after premature birth the premature infant may have some complications. A premature infant can have an immature respiratory system, making it difficult for the infant to breathe. Some infants' lungs lack surfactant. This substance ensures that the lungs can expand and contract. If this substance is absent, infants may develop respiratory distress syndrome [22].

The average resting respiratory rates for birth to 6 weeks is between 30 - 60 breaths per minutes (BPM), while for an adult this is between 12 - 20 breaths per minutes [3].

Breathing pathologies are one of the earliest indicators of physiological distress. If the respiration rate of a premature infant is abnormal, there may be a breathing disorder. Breathing disorders can be identified by respiration monitoring. Examples of altered breathing respiration are tachypnea: high breathing rate, bradypnea: low breathing rate or phase of apnea [4],[5]. Apnea has traditionally been defined as breathing pauses that last for longer than 20 seconds [17], [18]. To be able to make regular rhythmic breathing, a patented airway, central respiratory drive and adequate functioning of the respiratory muscles are required. Apnea is thought to be secondary to immaturity of brainstem centers that regulate breathing. The incidence of apnea of a premature infant is inversely related to gestational age. If the premature infant has a postmenstrual age around 37 to 40 weeks, it is usually solved. Apnea can be subdivided into three subgroups: obstructive apnea, central apnea and mixed apnea. Obstructive apnea means that the infant tries to breathe, but the airways are blocked so the infant gets no airflow. The chest is still moving up and down, because the infant tries to breathe. Obstructive apnea may be due to a lack of coordination of the upper respiratory tract muscles. These muscles are involved in keeping the airways open. They may collapse by the negative airway pressures generated during inspiration. Central apnea means that the apnea comes from a stop in the breathing center in the brain. As a result, the nasal airflow and breathing efforts cease simultaneously. Finally, mixed apnea is a combination of central and obstructive apnea. This is the most common apnea by small premature infants. Obstructive apnea occurs approximately for 10% to 25% of cases, central apnea occurs for approximately 10% to 25% of cases and mixed apnea occurs approximately for 50% to 75% of cases in premature infants. As the apneic episodes lasts longer, the proportion of mixed apnea-type events will progressively increase [17], [18]. A typical example is shown in figure 2.2.

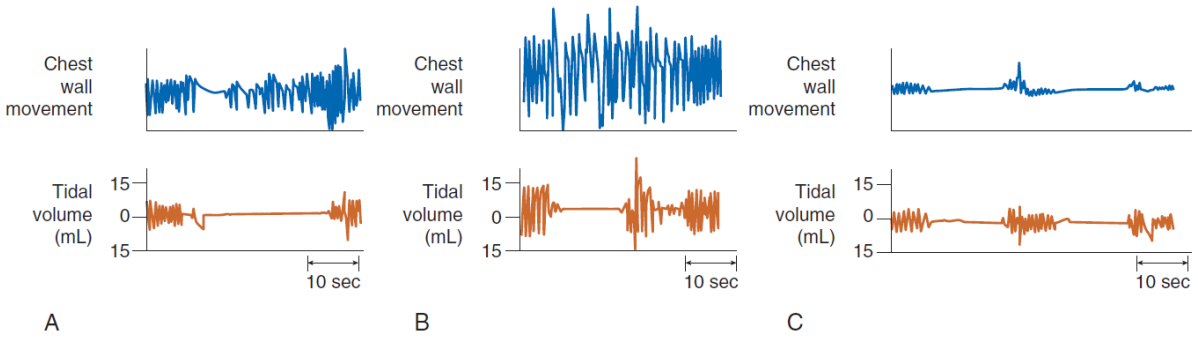

Figure 2.2: (A) Mixed apnea: consist of obstructed inspiratory efforts as well as a central pause, (B) Obstructive apnea: breathing efforts continue, although no nasal airflow occurs. (C) Central apnea: the nasal airflow and breathing efforts cease simultaneously [18].

2.2 Devices in a NICU

In figure 2.3 a picture can be seen of the NICU with (A) the incubator, (B) respiratory support, and the (C) monitor. An incubator is a special bed for a premature infant where the infant is provided with the right temperature and humidity. It is important that the incubator provides the ideal environment conditions, because the skin of a premature infant is not fully developed, so a lot of heat and moist is lost through the skin. The temperature that is necessary inside the incubator depends on the gestational age and illness [11].

Figure 2.3: A photo of the NICU, showing the incubator (A), respiratory support (B) and the monitor (C) [6].

Infants who do not yet have well-developed lungs get breathing support. An example of a breathing support is using a ventilator mask. The mask is attached behind the head of the infant with a band and is connected to the oxygen supply. Extra oxygen is administered through the nose with a certain flow rate. The infant is monitored by Electrocardiography (ECG). Three electrodes are attached to the infant's chest. An ECG registers the electrical signal from the heart. The heart rate can be determined from this. The respiration rate of an infant can also be monitored by the same electrodes. Two electrodes are placed on either side of the chest above and below the insertion of the diaphragm, see figure 2.4. Through the drive electrodes a high frequency ac current is injected into the tissue. The ac current causes a potential difference across these drive electrodes. The potential difference between the drive electrodes is related to the resistivity of the tissue. The resistivity can be determined by measuring the potential difference and the current that flows through the tissue. The impedance level of air is much higher than tissue. So, the air-to-tissue ratio will increase by inhalation and the electrodes will detect an increase in impedance [14],[22]. From the periodicity in this signal the respiration rate can be determined. If no signal is received, an alarm will sound and a nurse will intervene quickly. Furthermore, oxygen saturation is measured with a light sensor that detects differences in absorption of light that are related to the oxygen saturation of the blood. The temperature of the infant can be measured by using a thermometer. This thermometer can be put in the diaper [19].

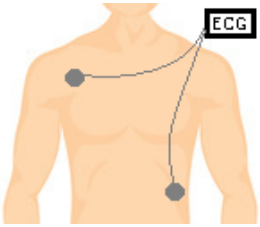

Figure 2.4: Sketch of the position of the two electrodes for measuring the respiration rate with ECG.

Determining the respiration rate with ECG had some disadvantages. The signal for the respiration rate of the infant can be disturbed by motion or cardiac artifact. Furthermore, if the airway is obstructed the chest still moves, making it seem like the infant is breathing [14]. Also, the attachment of the sensors to the infant's body induces stress and discomfort. Moreover, by frequently placing and removing the adhesive electrodes on premature infants leads to epidermal stripping and skin disruption, because the electrodes-dermis junction is stronger than the bond between the epidermis

and dermis. This is also the major cause of skin breakdown in NICUs [13]. Therefore, currently research is being conducted for contactless monitoring of respiration.

2.3 Contactless Monitoring of Respiration

Contactless monitoring of neonates using cameras has been done before and, in this section, the main setups that are used are described.

2.3.1 Other Studies

2.3.1.1 Research of University of Oxford

Figure 2.5: Monitoring equipment showing a mannequin inside the study incubator in the Oxford NICU [20], [21].

At the John Radcliffe Hospital in Oxford, research was performed to obtain continuous estimates of heart rate, respiration rate and oxygen saturation for infants nursed in incubators [20], [21]. 30 premature infants of less than 37 weeks of corrected postmenstrual age were monitored for up to four consecutive days. In figure 2.5 the setup to monitor the vital signs of these premature infant can be seen. A hole with a diameter of 3 cm was cut in the top of the incubator to get a good view with the video camera. The camera was mounted at the end of arm to minimize the disturbance to the care of the infant. The video camera (JAI AT-200CL, JAI, Glostrup, Denmark) with three separate CCD sensors (Sony ICX274AL) was used to measure red, green and blue light intensity independently. An area of exposed skin on the subject's face were selected: the location of the patient's face was detected using image segmentation, from [10]. Regular frequencies were sought in a signal which was considered to be stationary over the period of analysis. The dominant frequency in the reflected signal was the cardiac frequency, as a result of the changes in color and volume of superficial vessels with each cardiac cycle. The low frequency amplitude variations of the camera reflected signal from the subject Region Of Interest (ROI) were mainly caused by breathing-related motion. These breathing related amplitude variations were extracted with a band-pass filter.
The limitations of the technique are major changes in lighting conditions in the NICU, that effect the mean variation in the infant's activity patterns that can cause motion artifacts and the lack of visible skin area then no signal can be acquired. This causes a disruption of the determination of the respiration rate. It was possible to monitor the respiration rate continuously in the NICU. The accuracy was good enough to use this method in clinical settings.

2.3.1.2 Research of RWTH Aachen University

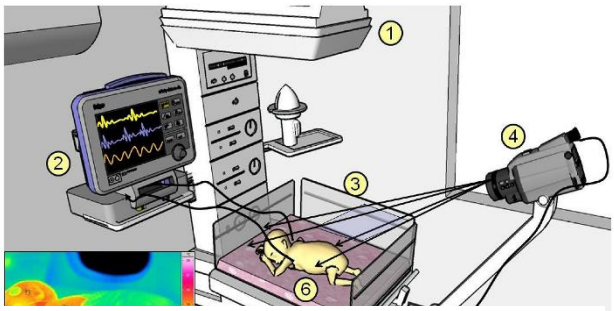

Figure 2.6: Schematic of the experimental setup of measuring the respiration rate of a premature infant. (1) radiant warmer bed, (2) bedside monitor, (3) camera field of view, (4) IR thermal camera. This camera was located 70 – 80 cm from the infant and was connected to the IR acquisition/analysis workstation (5) and (6) is the infant under NIRT imaging [8].

In Aachen research using infrared thermography imaging was conducted [8]. For this investigation seven premature infants with a median gestational age of 29 weeks were measured. In figure 2.6 the schematic setup can be seen. A VarioCAM HD head IR camera was used. The respiration rate was measured by measuring the temperature change in the nasal region. The thermal images were examined at different points in time. The frames that contained information from respiration in the ROI were selected. The time-varying signals from each point in the ROI were averaged and continuous wavelet transform (CWT) was applied to finally

determine the respiration rate. Though the setup could measure respiration in an open bed, the setup still needs improvement: such as automatic ROI definition and automatic calibration. Further, due to variation in background temperatures, the IR imaging device and the method itself still face drift problems. This requires improvements in image processing and boundary detection of the nasal region separated from the rest of the imaging scenario. Despite the limited number of measurements, the results of these measurements provide a good basis for further investigation. Moreover, the method that is discussed in this paper is an effective quantitative technique to measure the nasal symmetrical air-flow pattern in premature infants. This study conclude that this is a promising technology to measure the respiration rate of a premature infant.

In [13] the same setup was used, but with an algorithm that could automatically select the ROIs for detecting the respiration rate. Eight premature infants were monitored with a gestational age of 32 ± 4 weeks and a postnatal age of 27 ± 19 days. Some patients lied in the incubator and some in an open bed. Each infant was measured two times for 5 minutes on each side of the incubator/open bed. For the infants lying in the incubator the left or right porthole was opened to do the measurement. The former techniques only works if the nose is clearly visible in the image and it fails when the nose is outside the field of view of the camera. In this paper another technique was used to detect the respiration rate with a thermal camera. A grid was laid over the image with each grid cell representing one ROI. For each ROI the respiration signal and respiration rate were extracted. The ROIs with the best results were automatically selected and this information was fused in order to get robust estimations of the respiration rate. The respiration rate was successfully detected in clinical conditions. This shows that, infrared thermography is a promising alternative for current monitoring technologies in neonatal care. But this technique also has some limitations, it is sensitive for motion artifacts and it is mostly detecting respiration motion or a mix of respiration motion and flow [15]. Thus, the next aim should be to integrate a motion analysis algorithm capable of detecting motion noise inside the incubator, including patient movement, nursing interventions or parental touch.

2.3.2 Studies in MMC Veldhoven

2.3.2.1 Research of Ilde Lorato

In the research from RWTH Aachen University a bulky and expensive IR camera was used for detecting respiration flow. Therefore, Lorato et al. [15], choose to use a thermopile array and an ROI detection method that does not require facial landmarks. Thermopile arrays consist of multiple thermopile sensors and are constituted by thermocouples in series. The costs and the dimensions of a thermopile array are smaller.

This technique has been tested on multiple healthy adult subjects. The feasibility of detecting respiration with a thermopile array was analyzed for typical respiration conditions, oral/nasal breathing and different respiration rates. To mimic real-world applications, several other factors like distance from the sensor and orientation have been considered. After the videos were collected and pre-processed the data was analyzed with Matlab. The pixel with the greatest periodic variation overtime was selected and the respiration rate could be extracted in the frequency domain. This method allows to automatically select the ROI by discriminating between the pixels that output noise and flow-induced signals. The thermopile array loses accuracy at higher distances due to the low resolution of the sensor. Further, if the respiration rate is increased, the exhalation lasts shorter and this will decrease the heat transfer. It turned out that if the subject is lying with the side of the head on a pillow and the camera was positioned above the subject, this gave better results than if the subject was filmed in the frontal position. This is because the pillow was also heated during the exhalation. Besides, there is a delay in detecting a sudden change in respiration rate pattern.

Summarized, the respiratory flow in a lab setting could be measured with a low-cost thermopile-array. Also, no facial landmark detection was needed. Further development for the thermopile-array is an attractive alternative for expensive IR camera. Therefore, Ilde developed the setup further, using a

FLIR camera using a similar post-processing technique as in the thermopile. The FLIR has a higher resolution. The next question was if it can be used inside an incubator.

2.3.2.2 Research of Ineke Honings

A setup for simulating the neonatal flows was developed, using an artificial lung in an incubator. The artificial lung measurements were done with a low resolution FLIR Lepton 2.5 thermal camera for typical variations corresponding to neonatal breathing. Multiple tests were performed in this study, mimicking neonatal breathing by creating a flow out of the artificial lung. The measurements of respiration rate but in particular measurements quality and robustness, were performed in various incubator conditions.

It was possible to measure the respiration rate if the other parameters kept constant. However, the used ventilator was not good enough to simulate the breathing pattern of a premature infant, because the temperature of the air flow of the ventilator was varying 2°C. Moreover, the angle of the respiration relative to the snuggle matters a lot. The smaller the angle, the lower the amplitude of respiration. Next, the thermal camera was positioned on a tripod next to the incubator with an open porthole, tested on a small group of premature infants. This technique is only suitable for infants who were breathing without a ventilator mask, as then the flow due to respiration can be detected. Using a breathing mask, though thought to also show a temperature variation this did not result in a detectable temperature difference due to breathing [1].

3. Measuring Method

The respiration rate of a premature infant can be determined in 2 ways with a thermal camera. The first way is to measure the temperature difference at the nostrils during inhalation and exhalation. The second way is to monitor the thorax movement. In this project the focus is primarily on the thorax movement of an infant. To prepare for clinical measurements the best camera position needs to be determined. Because it was not possible to test on neonates, a simulator of thorax motion was developed.

3.1 Specifications

To simulate the movement of the thorax of an infant, typical values of the breathing motion are required. The moving part of the setup must have around the same temperature as the infant. A normal body temperature is between 36.5 °C and 37.5 °C. Furthermore, the amplitude of the thorax movement during inhalation and exhalation must be similar to human and neonatal breathing.
In [16] research was conducted regarding the inhaled tidal volume of an infant. This is between 4 and 6 mL/kg. The volume of air that is present in the lungs at the end of passive expiration of a premature infant is FRC = 24 mL/kg, FRC means Functional Residual Capacity [7]. In order to approximate the difference in the expansion and the contraction of the thorax during inhalation and exhalation, it is assumed that a lung is spherical. The volume of the sphere can be calculated with $V = \frac{4}{3}\pi r^3$, with V the volume and r the radius of the sphere. For convenience 4 mL/kg is chosen for an infant with a weight of 1000 g. The radius of a lung at the end of passive expiration is then $r = 2.62$ cm and the radius of a lung after inhalation is $r + \Delta r = 2.76$ cm. Thus, the amplitude is $\Delta r = 0.14$ cm. But since the lungs are not spherical the difference in the expansion and the contraction of the thorax is estimated at 1 mm. For an adult person the FRC is around 5 L and the inhaled tidal volume is 0.4 L This gives an amplitude $\Delta r = 0.4$ cm, thus the amplitude is estimated at 3 mm.
The abdominal circumference of a premature infant with gestational age of 24 is 20 cm [12]. Thus the width of the surface of the abdomen is 10 cm.

3.2 Setup

Various setups have been considered to simulate the movement of the thorax of an infant. The first set-up was the one previously used by Ineke [1]. In figure 3.1A a picture of the setup from Ineke can be seen, with (A) the incubator, (B) the mattress, (C) the snuggle, (D) the ventilator, (E) the artificial lungs, (F) the camera, (G) the laptop with Matlab and (H) the monitor. The limitations of this setup are that the availability of the setup was limited, the temperature is very close to the environment temperature and the temperature is not constant, it varies with 2°C.
The second setup was developed using a warm water bottle. In figure 3.1B the setup is shown. The thermal camera (A) was mounted on the mounting arm (B) and connected to a laptop via a USB cable. The mounting arm was attached to an open baby bed (C). A Babybe bionic mattress (D) was placed in this bed. The Babybe bionic mattress was attached to the manual ventilator (E) with tape, because they both had a different connection. A water bottle (F) was placed on the Babybe mattress with warm water at approximately 40 °C. A snuggle (G) was placed over the bottle. The limitations of this setup are that the movement of the bottle does not properly simulate the thorax movement of the infant and the respiration rate was not constant, because of the manual ventilation.
The third setup was designed with balloons. The balloons needed to be inflated manually with a manual ventilator. In figure 3.2A a schematic setup is shown with (orange) the balloons, (light green) a blanket, (dark green) the manual ventilator, (red) the warm water bag, (purple) a blanket, (dark blue) the thermal camera, (grey) the mounting arm and (light blue) the mattress of the open bed. The limitations of this setup are that the respiration rate is not constant, furthermore the balloon loses elasticity over time. Finally, the heat is not well distributed, because the highest temperature will be below the balloons.

The fourth setup uses an engine that rotates a metallic cylinder with an eccentrically positioned axis. In figure 3.2B the setup with the engine is shown with (purple) the engine, (dark green) the rotating cylinder with an eccentrically positioned axis, (brown) wooden board, (red) the warm water bag, (dark blue) the thermal camera, (grey) the mounting arm and (light blue) the matrass of the open infant bed. The simulated respiration rate of this setup is constant and the heat source is moving, this gives a better simulation of the thorax movement of the infant. The last setup is chosen, because this was the best setup with the least limitations of the four possible setups and that could be developed within the given time frame.

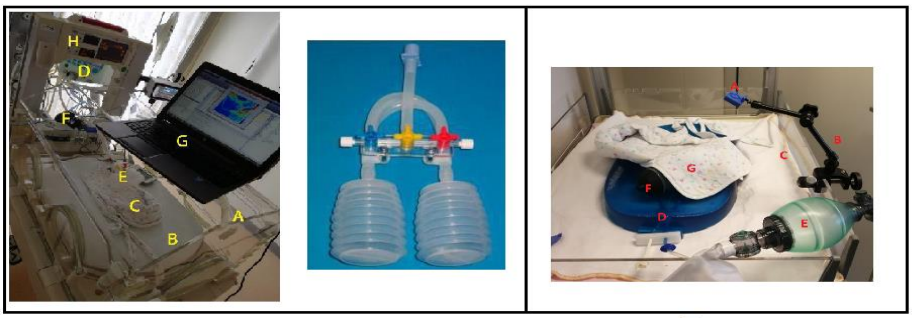

Figure 3.1: Figure (A) shows the setup of Ineke that simulates neonatal flows. In this picture (A) is the incubator, (B) the mattress, (C) the snuggle, (D) the ventilator, (E) the artificial lungs, (F) the FLIR Lepton 2.5 camera, (G) laptop with Matlab and (H) the monitor of the incubator [1]. In figure (B) the setup with the water bottle can be seen. In this picture (A) is the thermal camera, (B) the mounting arm. (C) an open baby bed, (D) a Babybe bionic mattress, (E) the manual ventilator, (F) the water bottle and (G) the snuggle (G).

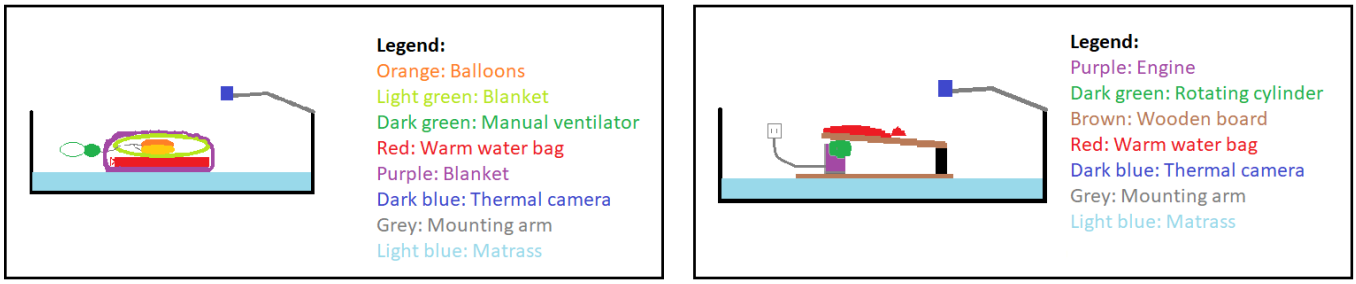

Figure 3.2: Figure A shows the setup with the balloons, with (orange) the balloons, (light green) a blanket, (dark green) is manual ventilator, (red) the warm water bag, (purple) a blanket, (dark blue) the thermal camera, (grey) the mounting arm and (light blue) the matrass of the open infant bed. In figure B the setup with the engine is shown, with (purple) the engine, (dark green) the rotating metallic cylinder with an eccentrically positioned axis, (brown) wooden board, (red) the warm water bag, (dark blue) the thermal camera, (grey) the mounting arm and (light blue) the matrass of the open infant bed.

3.2.1 Detailed Explanation of Setup

The movement of the thorax of the infant was simulated with an engine that rotates a metallic cylinder with an eccentrically positioned axis, which is called 'the eccentric'. This eccentric pushes a wooden board up and down in a sinus movement, see figure 3.3. A warm water bag was put on this wooden board, to mimic the body temperature of an infant.

The engine was connected to the power line through a transformer to reach a voltage of 12 V. The eccentric was attached to the engine. The eccentric was made of metal and has a hole of 4 mm from the center of the disc. This will cause the eccentric to make a periodic movement. The eccentric pushes against a green block, see pictures 5 and 6 of figure 3.3. This block was made of a material that slips well; this reduces friction. This green block was attached to a wooden board. On the wooden board, there was a warm water bag, attached to the wooden board with 2 Velcro strips. The warm water bag has a volume of 600 ml and was filled with water with a temperature of approximately 40 °C, see picture 1 – 4 of figure 3.3 for different views.

Picture 1: Side view 1

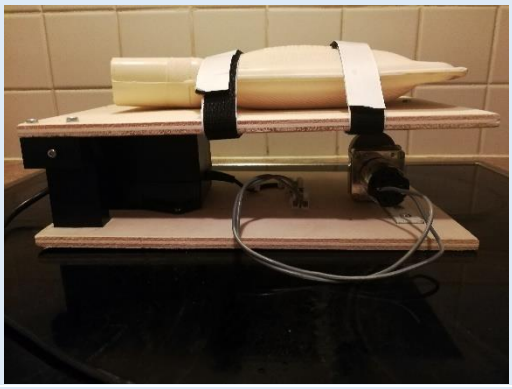

Picture 2: Side view 2

Picture 3: Front view

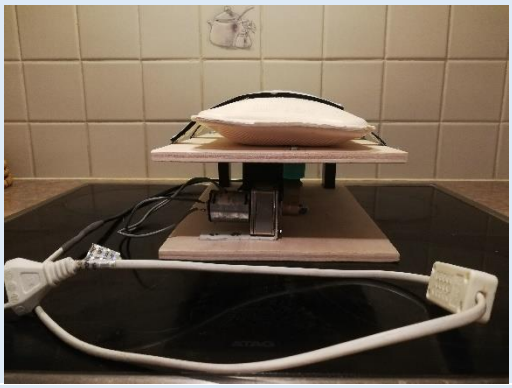

Picture 4: Top view

Picture 5: Front view of the engine

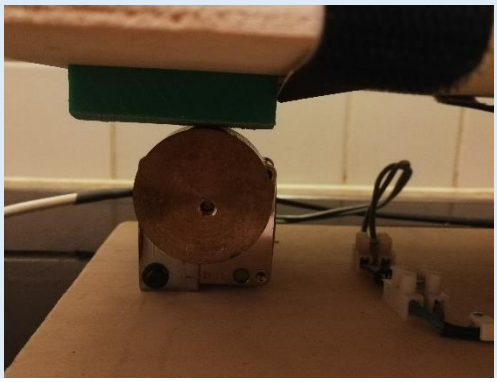

Picture 6: Side view of the engine

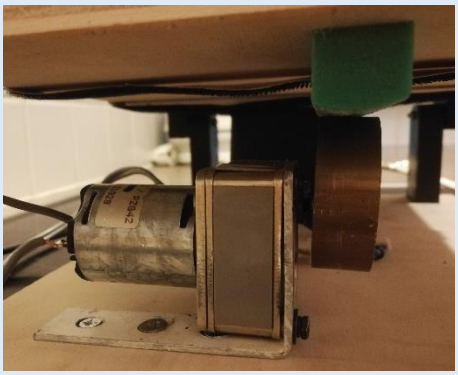

Figure 3.3: Pictures 1-4 show the side, front and top view of the simulator and pictures 5-6 show the front and side view of the engine of the simulator.

The dimensions of the warm water bag are 26 x 15 x 5 cm. The setup has dimensions of 30 x 20 x 14 cm. The amplitude of the end of the wooden board was 8 mm. If the warm water bag was placed on the wooden board, then the amplitude was 7 mm. Different amplitudes could be simulated by placing the warm water bag at different locations on the wooden board. Furthermore, the engine can be set at different speeds, so that different respiration rates could be simulated. The frequencies of the engine can be set from 0 BPM to 80 BPM. The speed of the engine decreases as the weight on the wooden board increases. In short, if the weight is on the end of the wooden board, the part with the highest amplitude, the engine will run slower at the same set speed than if the same weight is laid at the beginning of the wooden board, the part with

Figure 3.4: dc-dc adjustable step down voltage regulator module lm2596s. The dark red circle indicates the screw that need to be turns to change the speed of the engine.

the lowest amplitude. To change the speed of the engine an adjustable step-down voltage regulator was used. The speed could be varied by turning the screw indicated with a dark red circle in figure 3.4 with a small screwdriver. There was not enough time left to calibrate this adjustable step voltage regulator. As a result, the frequency was determined by counting and using a stopwatch.
The setup was placed in an open infant bed, see figure 3.5. The thermal camera was attached to the edges of this open infant bed with a mounting arm. The videos were recorded with the FLIR Lepton 2.5 camera, the same as used in the previous study (see section 2.3.2.2.). The Lepton camera was connected with an Acer Swift 3 laptop and will be explained in the next section.

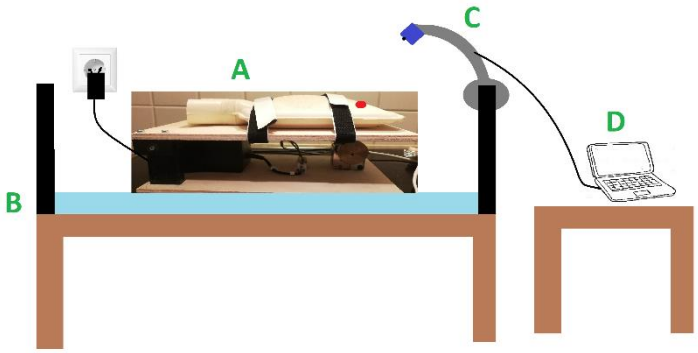

Figure 3.5: Schematic representation of the setup. With (A) the simulator, (B) The open infant bed, (C) the thermal camera with the mounting arm and (D) the laptop with Matlab.

3.3 Acquisition and Processing of Thermal Images

For acquisition of the thermal images in this setup the FLIR Lepton 2.5 camera was used. This is a low-resolution thermal camera with 60 by 80 pixels, has a sensitivity of 0.05 K and has a frame rate of 8.7 Hz. An Acer Swift 3 laptop with windows 10 was used to record and analyze the videos collected with the FLIR Lepton 2.5 camera. The Matlab scripts of Lorato [15] was used to analyze the data. First the videos were collected and pre-processed with Matlab. Then the pixel with the greatest variation was selected and the respiration rate could be extracted in the frequency domain. The main steps of the processing chain are summarized in figure 3.6. The processing chain was implemented in Matlab 2019.a and the data processing was performed offline. Details are explained below.

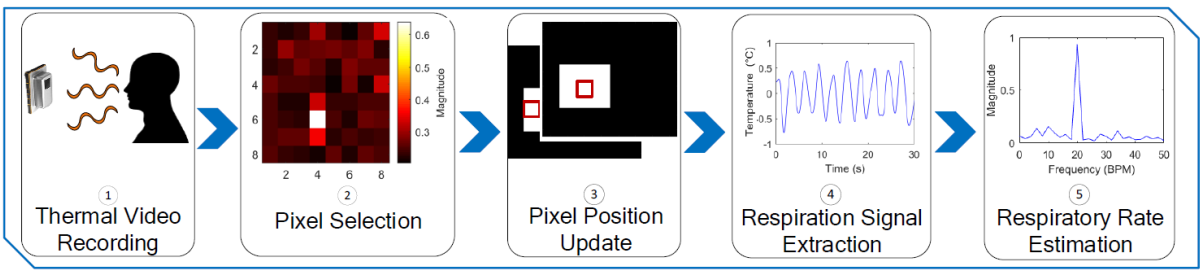

Figure 3.6: Block diagram summarizing the processing chain from image' acquisition to respiration rate extraction [15].

To control the camera and record the thermal videos the Matlab script called "acquisition" was used. At the beginning of each measurement the shutter was closed to reset all pixels in the camera. A video with an image of 60 x 80 pixels was recorded and saved on the laptop. The recording time of each measurement was 2 minutes. The Matlab script called "Comparison" compares multiple measurements with each other. The data was acquired using USB-connection and Matlab. Since the cameras do not support hardware triggering, the video will result in not having a constant frame rate and therefore interpolation was performed to create a uniformly sampled data set in the temporal dimensions with a sampling frequency of 10 Hz. To suppress thermal variations of the environment the spatial mean was removed. A sliding window approach with a window size of 15 seconds was used to process the videos. This means that after 15 seconds the first respiration rate estimate would be

available and then updated. The time lag was considered to be acceptable [15]. For each window, the pixels with a high correlation with the firstly chosen pixel with the highest peak in the normalized spectrum were automatically selected. The pixels' signals were filtered using a Butterworth bandpass filter from 40 to 80 BPM for each window. This range is a normal respiration rate for premature infants including also tachypnea. The respiration rate was determined by using the Fourier transform, see picture 5 in figure 3.6 for an example.
The results were analyzed by looking at the maximum amplitude change of the temperature in °C, the number of pixels involved in detecting respiration, the root mean square error (RSME) of the respiration rate and the signal to noise ratio (SNR). For each type of measurement that was repeated several times, the average and the standard deviation were taken. The amplitude, number of pixels and the SNR must be as high as possible and the RMSE must be as low as possible.
Before the data was analyzed for this setup, an expectation value for the respiration rate must be entered. The RMSE of the respiration rate calculates the error with respect to the expected respiration rate. If the respiration rate is constant, the RMSE should be zero. There are several reasons why the RMSE might not be equal to zero.
The first reason is that the expected respiration rate that has been entered beforehand is incorrect, as the respiration rate was determined by counting and timing it with a stopwatch, thus being inaccurate.
The second reason is the frequency resolution. We calculate the respiration rate with a sliding window approach with a window size of 15 seconds. This means that after 15 seconds the first respiration rate estimate would be available and then updated. The window will move 0.1 seconds and then the frequency was determined again. The sliding window approach is illustrated in figure 3.7A and B. In figure A can be seen how the window was updated and in figure B the determined respiration rates for both windows are given. The x-axis of the respiration rate is different between the figures A and C, and B and D, this is because the last window runs from 105 – 120 s. The frequency resolution is 4 BPM. Suppose the determined frequency is 40.5 BPM and the frequency resolution causes the frequency to be 38 BPM or 42 BPM an example can be seen in figure B. The line in this figure has some fluctuations and the frequency in figure D is constant. The two problems can cause an increase in the RMSE. Thus, if the RMSE is below 4 BPM, then the signal was considered correct.
The SNR of the signal of figure D will be higher than the signal of figure B, because the frequency is constant.

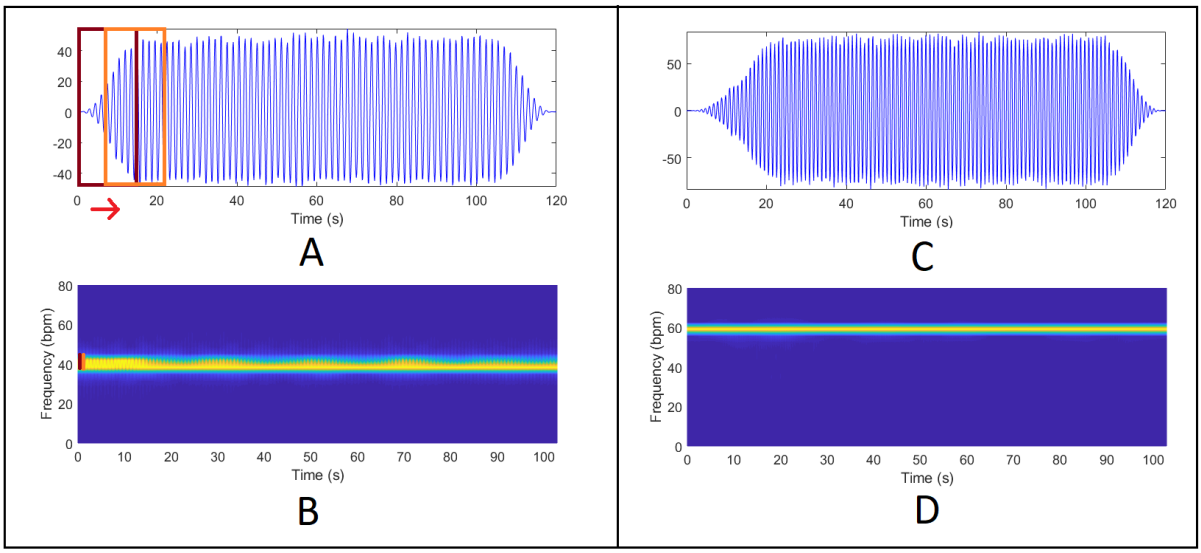

Figure 3.7: The time domain signals (A and B) and the frequency change over time (B and D) of two different examples are shown. In figure B the frequency change over time is not constant, it fluctuates and in figure D the frequency change over time is constant.

3.4 Determining the Test Setup

To test the optimal camera position, the angles could be varied in two directions, namely in the horizontal plane and in vertical plane. The angle in the horizontal plane was indicated by the symbol φ and the angle in vertical plane was indicated by the symbol θ, see figure 3.8A and 3.8B, respectively. In the horizontal plane the angle φ could be varied from 0° to 180°. The angle θ could be varied between 0° and 90°.

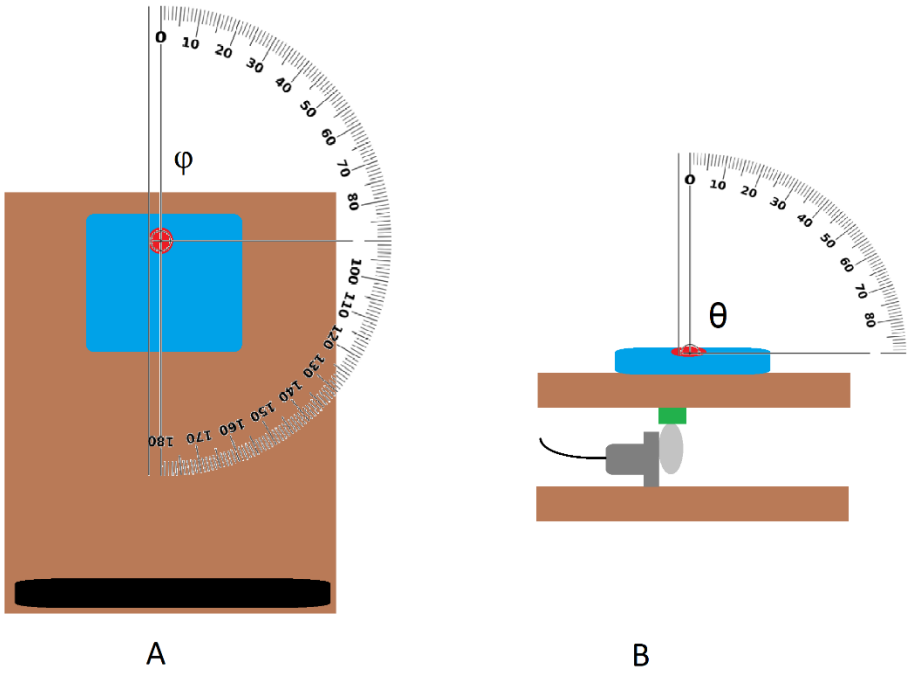

Figure 3.8: picture (A) shows the top view of the simulator showing how the angle φ was defined and picture (B) shows the front view of the simulator showing how the angle θ was defined, with (brown) the wooden board, (blue) the hot and cold pack, (red) the center of interest for the defining the variables, (black) the hinge and (grey) the engine with the rotating metallic cylinder.

The designed simulator was first tested with the thermal camera. In the first test, the simulator was filmed from the side view with a warm water bag and was attached to the wooden board with Velcro strips, see picture 1 from figure 3.9. The respiration rate was 60 BPM, the angle φ ≈ 90°, θ ≈ 90° and the distance was around 30 cm. In the second test, the simulator was also filmed from the side view, φ ≈ 90°, only now at an angle of θ ≈ 70°. The Velcro strips were removed, and a blanket was placed over the setup. In the third test, the simulator was filmed in the front view with a hot and cold pack instead of a warm water bag. The hot and cold pack was made of gel and could be heated using a microwave or warm water. Because the hot cold pack was less heavy than the warm water bag, the respiration rate was increased to 70 BPM. The distance was around 20 cm and the angle φ ≈ 0° and θ ≈ 70°. In the fourth test, the same measurement was performed as in test 3, the only difference was that a blanket was laid over the hot and cold pack.

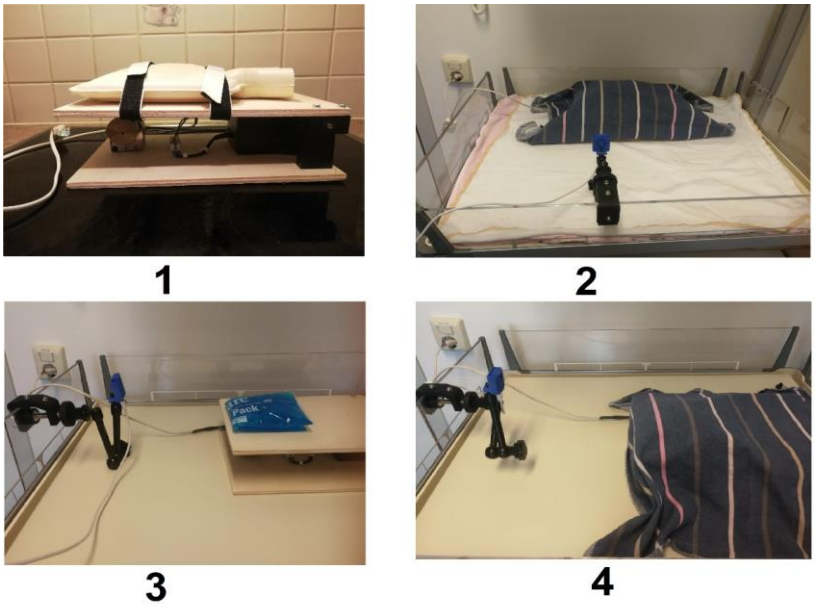

Figure 3.9: (1) Test measurement 1: side view, with a warm water bag and 2 x velcro strips, (2) Test measurement 2: side view, with a warm water bag without velcro strips and with a blanket, (3) Test measurement 3: Front view, with a hot cold pack and (4) Test measurement 4: Front view, with a hot cold pack and with a blanket.

In figure 3.10 the temperature images and the correlation images can be seen of all the four test measurements. The color yellow in the correlation images indicates a positive correlation and the color blue indicates a negative correlation with the signal of the pixel firstly chosen as the one with the highest periodic pattern. Thus, the color yellow, indicated with '1' in the legend, indicates that it moves with the same periodic pattern as the firstly chosen pixel and the color blue, indicated with '-1', indicates that it moves 180° out phase with the firstly chosen pixel. This method has the disadvantage that the firstly chosen pixel can influence the correlation images, causing that three the same measurements give different correlation images. In figure 1 of test 1 the temperature distribution and the correlation image can be seen of the warm water bag. At the angle of $\theta \approx 90°$ the bottom of the warm water bag was also filmed. As a result, the correlations at the top of the warm water bag are negative and at the bottom of the warm water bag are positive. The top and the bottom are therefore 180° out phase.
The second test, the simulator was also filmed from the side view only now at an angle of $\theta \approx 70°$. The Velcro strips were removed, and a blanket was placed over the setup. The bottom of the warm water bag and the region below the board was no longer seen by the thermal camera at an angle of $\theta \approx 70°$. This solves the problem of the two parts that were out of phase. This can be seen in figure 2 of test 2. There were still problems with the thermal videos. This is because the temperature of the water in the warm water bag was not homogeneously distributed. The edges of the warm water bag were made of thick rubber and as a result this part was hardly heated by the water. This can be seen in figure 1 of test 2.
In the third test, the simulator was filmed in the front view with a hot cold pack instead of a warm water bag. The distance was around 20 cm and the angle $\varphi \approx 0°$ and $\theta \approx 70°$. The temperature distribution of the hot and cold pack was better than the temperature distribution of the warm water bag. This can be seen in figure 1 and 2 of test 3. Also, the top part of the hot and cold pack gives a positive correlation.
In the fourth test, the same measurement was performed as in test 3, the only difference was that a blanket was laid over the hot and cold pack. This gives a better temperature distribution than test 3.

From the test setup can be concludes that the angles higher than angle θ = 70° are no longer representative for stimulating the movement of the chest of an infant. Further the hot and cold pack has a better temperature distribution than the warm water bag. Finally, the blanket gave an even more better temperature distribution. Thus, the rest of the measurements were therefore carried out with a hot cold pack with a blanket wrapped around the setup.

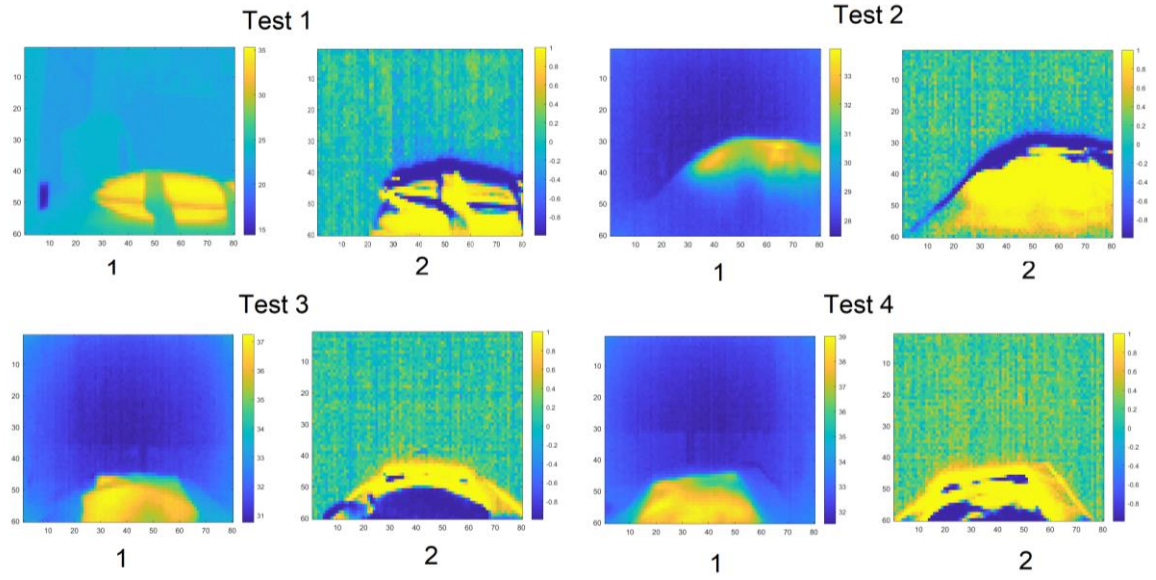

Figure 3.10: The temperature images (1) and correlation images (2) for all four test measurements.

3.5 Measurements Protocol to Test Different Conditions and Variables

With the setup discussed in section 3.2, different parameters could be varied to find out which position is best for determining the respiration rate (RR) of the thorax movement. The angle φ and θ, the respiration rate, the distance and the amplitude were varied. In table 3.1 the measurements are summarized. All videos have a duration of 2 minutes and all measurements were repeated three times. The average of these three measurements were taken. The temperature of the hot and cold pack varied between 37°C - 44°C. The hot and cold pack loses heat over time, therefore it had to be warmed up again a several times.

In measurement 1 the angles in the horizontal plane were varied from φ = 0° to 180°, with steps of 20°. The setup was symmetrical; therefore, measurements were only taken on one side.

In measurement 2 the angles in the vertical plane were varied from φ = 0° and 70°, with steps of 10°. This measurement was done for a fixed φ = 90° and φ = 180°. The angle θ was varied for two different angles φ to see if this would yield comparable results. These angles were chosen, because both angles view the movement at a different angle. At the angle of φ = 90°, the setup was filmed from the side, so that the movement was perpendicular to the camera. At angle φ = 180° the setup was measured from the rear, so that the movement was directed towards the camera.

Table 3.1: An overview of the different varied parameters and the fixed variables.

Measurement	Angle φ (°)	Angle θ (°)	Distance (cm)	RR (BPM)	Amplitude (mm)	Total measurements
1	0° - 180°	70°	20	70	7	30
2	90°, 180°	0° - 70°	20	70	7	48
3	180°	30°, 50°, 70°	20	42, 50, 61, 80	7	36
4	90°	70°	20 - 40	72, 69, 66	1, 3, 7	27

Further, in measurement 3 it was being investigated whether the respiration rate influences the results. The engine could be set at different speeds from 0 BPM to 80 BPM. Three mounting arms were used and adjusted to three specified angles, in order to prevent variation between the specified angles at different respiration rates. In figure 3.11 the side view and front view of the setup can be seen. The angle $\varphi = 180°$ was chosen, because the results from measurement 2 shows that $\varphi = 180°$ gave better results than $\varphi = 90°$.

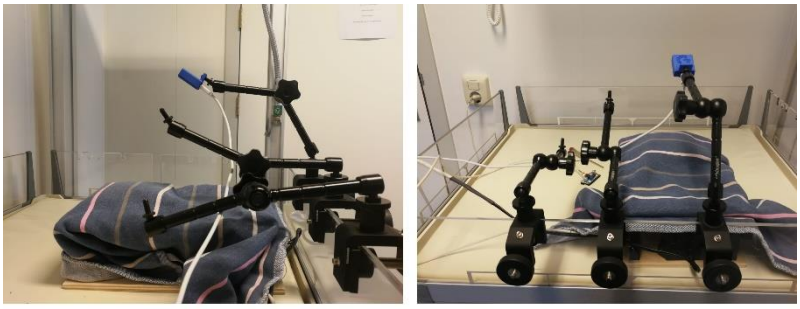

Figure 3.11: Figure (A) shows the side view of the setup of measurement 3 and figure (B) shows the front view of the setup of measurement 3. The mounting arms were set to the angle $\theta = 30°$, $\theta = 50°$ and $\theta = 70°$, respectively.

In measurement 4 the distance between the camera and the simulator was varied. The distance was varied between 20 cm to 40 cm, in steps of 10 cm. Also, the amplitude of the motion of the simulator was varied: 1 mm, 3 mm and 7 mm. Three distances were measured at each amplitude. In the first measurement, the hot and cold pack was placed at the end of the wooden board like all other measurements. The amplitude of the movement of the hot and cold pack was 7 mm. In the second measurement, the hot and cold pack was moved to the middle of the wooden board. This gives an amplitude of 3 mm. The third measurement the hot and cold pack was placed at the start of the wooden board, so the amplitude was 1 mm. This was to simulate between adult and expected neonatal breathing amplitudes of the chest. For an amplitude of 1 mm, 3 mm and 7 mm the respiration rate was 66 BPM, 69 BPM, 72 BPM, respectively. This is because the weight of the hot and cold pack was moved over the wooden board, making the engine run faster, at the same set position of the screw of the adjustable down voltage regulator. The speed could be changed again at the different positions, to keep the speed the same, but it was very difficult to find the right speed, because it was not calibrated. In order to prevent variation of the angle and distances between the measurements by different amplitudes, three mounting arms were used and adjusted for different distances. In figure 3.12 the setup is shown at different views. The simulator needed to be moved forward or backward for each mounting arm to get the correct distance and angle. In figures A and B this is set for a distance at 40 cm.

Figure 3.12: Figure (A) shows the side view of the setup of measurement 4 and figure (B) shows the front view of the setup of measurement 4. The mounting arms were set at the angle $\theta = 70°$ for different distances: 20 cm, 30 cm, 40 cm, respectively. The simulator needed to be moved forward or backward for each mounting arm to get the correct distance and angle. In figures (A) and (B) this was set for a distance of 40 cm.

In Measurement 1 - 3 the chosen amplitude was kept constant at 7 mm instead of an amplitude of 1 mm of a thorax movement of an infant or 3 mm of the thorax movement of an adult, which was explained in section 3.1. The reason is that in the first three measurements it was investigated whether the thermal camera can still pick up the signal of the movement at different angles and respiration rates. For that a large signal was wanted to investigate the influence without already being the noisy region. This amplitude was adjusted in measurement 4.
The data of each measurement wherein a variable was varied will be plotted in four graphs. All the four plots have the same x-axis with the varied variable and the y-axis of the graphs are the amplitude of the temperature change °C, SNR in dB, the number of pixels involved in respiration and the RMSE in BPM.

4 Results

In this chapter, the results of the measurements as discussed in chapter 3 are presented. The results will be discussed in chapter 5.

4.1 Vary the Angle φ

In figure 4.1 the temperature images can be seen for the setup with the hot cold pack with the angle φ varied from 0° to 180°, with steps of 20°. Because of the position accuracy the amount of hot and cold pack that came into the cameras view is different by each angle and this has influences on the number of pixels involved in detecting respiration rate and the SNR. The results of the measurements are shown in figure 4.2.

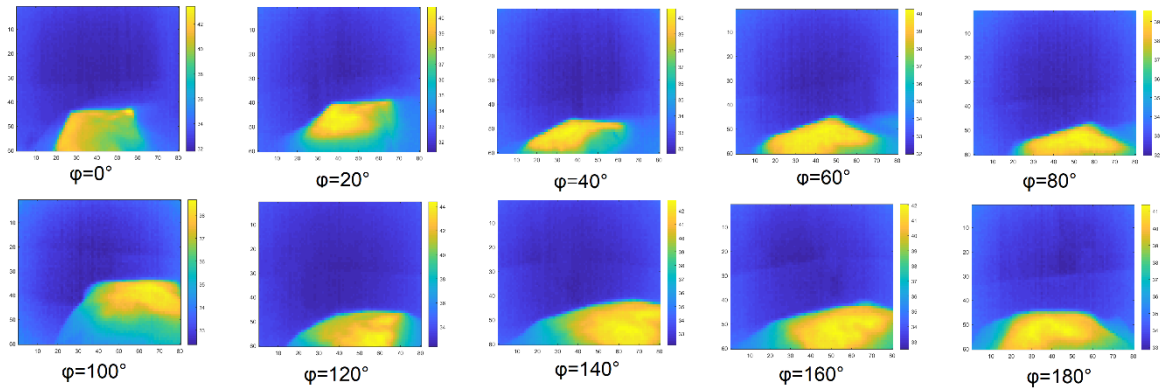

Figure 4.1: The temperature images for φ were varied from 0° to 180°, with steps of 20°. The hot cold pack had a temperature between 38°C - 44°C. The other variables were fixed: the respirate rate was 70 BPM, the distance was 20 cm, the angle θ = 70° and the mean height difference was 7 mm.

In figure 4.2A the maximum amplitude change is plotted against angle φ. The highest amplitudes can be seen at the angles 120° to 180° and at the angles of 20°, 40° and 100° the amplitudes are the smallest. The warm water bag was reheated several times during measurement 1, at φ = 0°, φ = 60°, φ = 120°. This can be clearly seen in the results of the amplitude. The amplitude decreases as the temperature drops in the hot and cold pack.
In figure 4.2B the number of pixels is plotted against angle φ. The number of pixels varies between 400 and 1400 pixels. The angle φ = 0° has a large standard deviation and angle φ = 100° has many more pixels than the other angles. It was expected that φ = 100° has more pixels than the other measurement, because in the temperature image of φ = 100° in figure 4.1 can be seen that a larger part of the heat source is visible in this measurement. This is due to inaccuracy in positioning.
In figure 4.2C the RMSE of the respiration rate in BPM is plotted against angle φ. The RMSE is below 4 BPM.
In figure 4.2D the SNR is plotted against angle φ. The bigger the angle φ, the higher the SNR.
My conclusion of this measurement is that the best angles are between φ = 120° to φ = 180°.

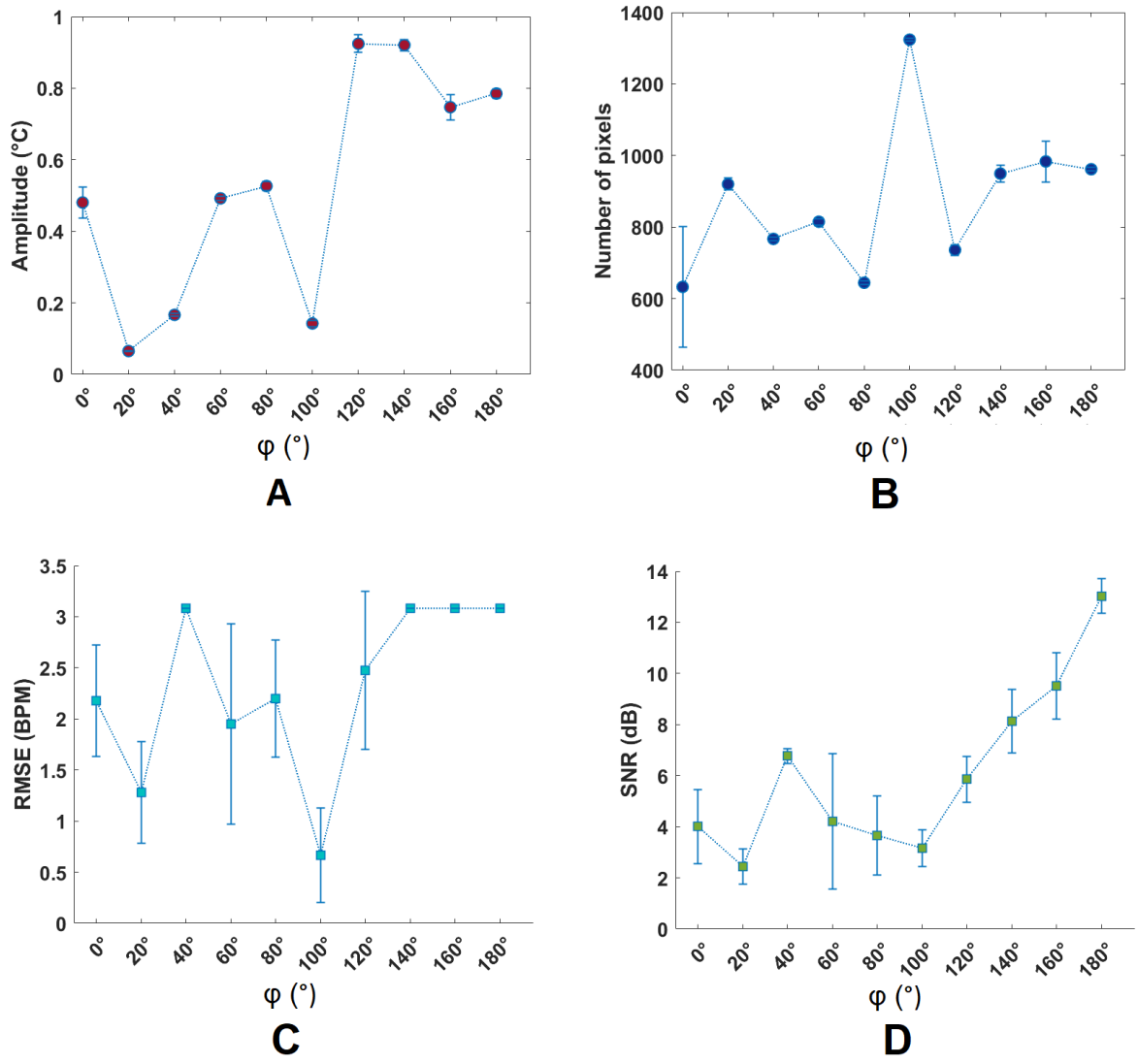

Figure 4.2: The results of measurement 1. The angle φ was varied from 0° to 180°, with steps of 20°. The other variables were fixed: the respirate rate was 70 BPM, the distance was 20 cm, the angle θ = 70° and the mean height difference was 7 mm. Figure (A) shows the results of the amplitude in ℃, figure (B) shows the number of pixels, figure (C) shows the RMSE in BPM and figure (D) shows the SNR in dB.

4.2 Vary the Angle θ

In the Appendix in figure A.1 and figure A.2 the temperature images can be seen for the setup with the hot cold pack with the angle θ varied from 0° to 70°, with steps of 10°. This measurement was done for a fixed φ = 90° and φ = 180°. The results of the measurement with a fixed φ = 90° and φ = 180° are shown in figure 4.3.

In figure 4.3A the maximum amplitude change in the temperature is plotted against angle θ. The amplitudes for φ = 90° at θ = 0° and θ = 10° are the highest. The amplitudes for φ = 180° appears to increase by increasing the angle θ, but this is due to the fact that the temperature of warm water bag at the smaller angles was lower than the temperature of the warm water at higher angles was higher, this can be seen at the temperature images. In addition, the heat difference of the environment and the heat source becomes larger as the angle θ becomes larger, because more background comes into the view. Further, the temperature images of φ = 90° show that the warm water bag had a lower temperature than the temperature images of φ = 180°.

Moreover, in figure 4.3B the number of pixels varies between 500 and 1600 pixels. The relation between the number of pixels and the angle θ for the angle φ = 90° and φ = 180° looks similar, but the number of pixels is higher of φ = 180°. Both angle of φ shows an increase in the number of pixels from θ = 0° to θ = 50° and decrease in the number of pixels from θ = 50° to θ = 70°.
Further, both measurements give a RMSE below 4 BPM for all angles θ, this can be seen in figure 4.3C. The highest RMSE is of φ = 90° at angle θ = 40° and of φ = 180° are at angle θ = 50° and θ = 60°, but the RMSE is still smaller than 4 BPM.
Finally, in figure 4.3D the SNR of φ = 90° is on average between 6 and 8 dB. The angle at θ = 0° has a SNR that is almost 2 times larger than the average and angle θ = 40° has a SNR that is 2 times smaller than the average. The SNR of φ = 180° is for angle θ = 0° to θ = 30° high and for angle θ = 40° to θ = 70° low. The SNR values from both angles φ from angle θ = 50° to θ = 70° are around 7 dB. The angles from θ = 0° to θ = 40° give different results.
My conclusion of this measurement is that the best angle φ = 180° gives best results at angle θ = 10° to θ = 30°.

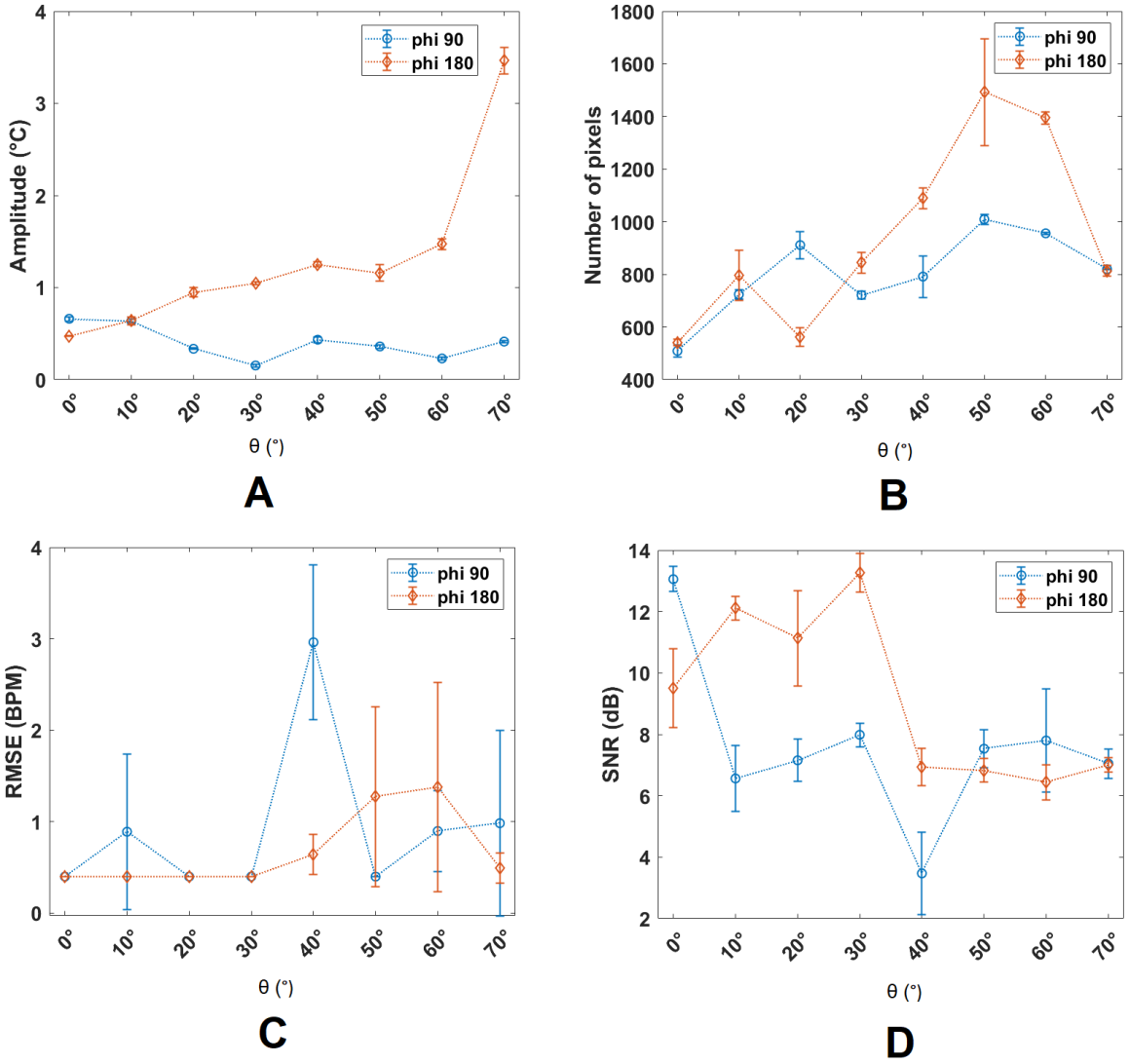

Figure 4.3: The results of measurement 2. The angle θ was varied from 0° to 70°, with steps of 10°. This measurement was done for a fixed φ = 90° and φ = 180°. The other variables were fixed: the respirate rate was 70 BPM, the distance was 20 cm and the mean height difference was 7 mm. Figure (A) shows the results of the amplitude in °C, figure (B) shows the number of pixels, figure (C) shows the RMSE in BPM and figure (D) shows the SNR in dB.

4.3 Vary the Respiration Rate

The respiration rate was set at 42 BPM, 50 BPM, 61 BPM and 80 BPM. Each chosen respiration rate was measured at angle θ = 30°, θ = 50° and θ = 70°. In the Appendix in figure A.3 the temperature images with a respiration rate of 42 BPM, 50 BPM, 61 BPM and 80 BPM can be seen for the setup. The results of the measurement for different respirations rates and angle θ can be seen in figure 4.4.

In figure 4.4A the maximum amplitude change can be seen. The amplitude mean value remains for all four respiration rates and three angles θ between 1.1°C and 1.4°C. It can be observed that at θ = 50°, the respiration rate 50 BPM and 80 BPM show a high standard deviation.

In figure 4.4B the number of pixels of all the respiration rates have almost the same relation. The number of pixels involved in detecting respiration are for θ = 70° for all the respiration rates higher than the other angles. The respiration rate of 80 BPM has lower number of pixels then the other respiration rate. The number of pixels varies between 500 and 1800 pixels.

In figure 4.4C the RMSE is below 4 BPM and the lines are constant for each respiration. For some respiration rate the RMSE is higher, this is since the expected value was incorrectly estimated.

In figure 4.4D the SNR are low for respiration rate 42 BPM, 50 BPM and 80 BPM and high for 61 BPM. The SNR for respiration rate 42 BPM, 50 BPM and 80 BPM is between 2 and 5 dB and the SNR for the 61 BPM is increasing by increasing the angle θ.

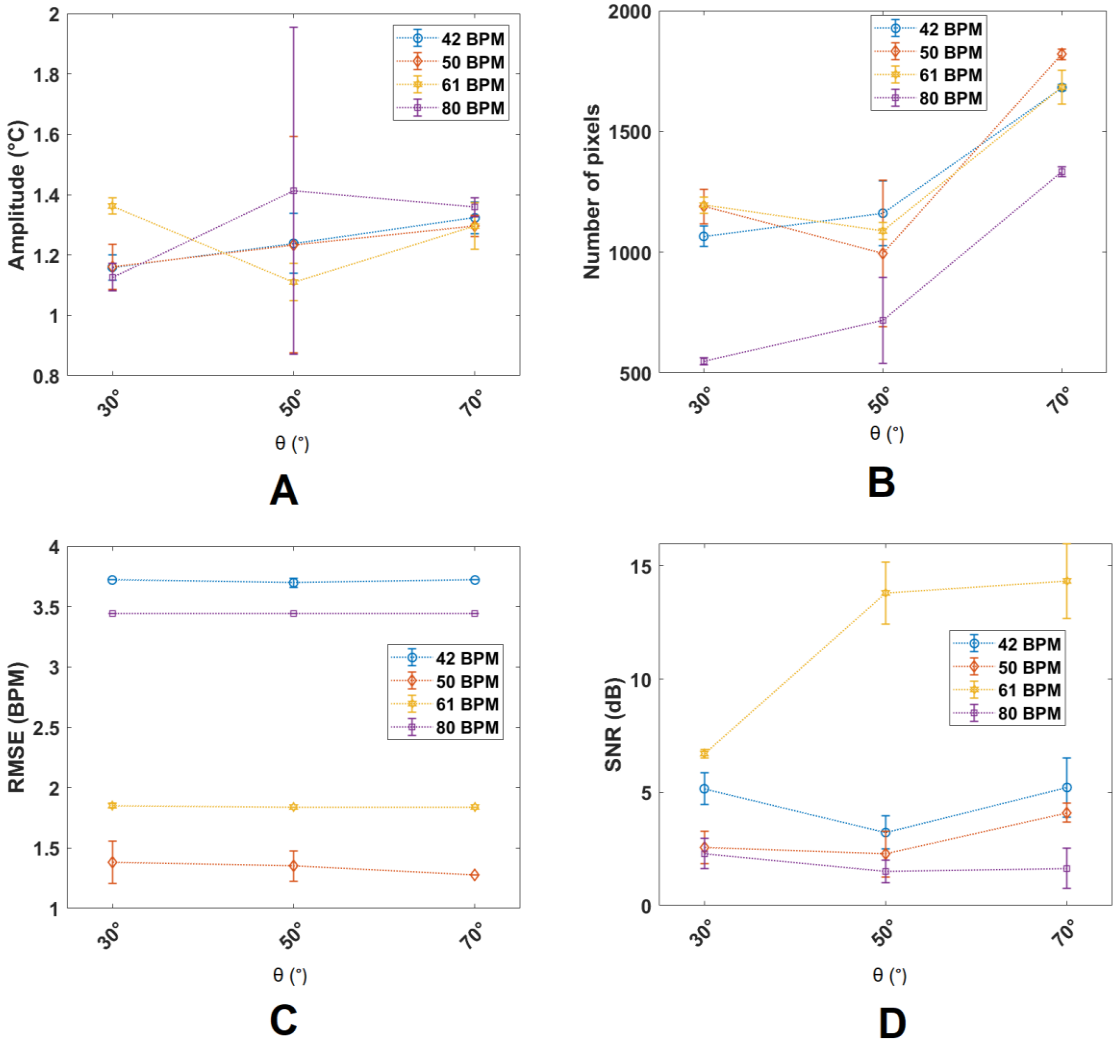

Figure 4.4: The results of measurement 3. The angle θ = 30°, 50° and 70° and the respirate rate were varied: 42 BPM, 50 BPM, 61 BPM and 80 BPM. The other variables were fixed: φ= 180°, the distance was 20 cm and the mean height difference was 7 mm. Figure (A) shows the results of the amplitude in °C, figure (B) shows the number of pixels, figure (C) shows the RMSE in BPM and figure (D) shows the SNR in dB. The hot cold pack had a temperature between 36°C - 42°C.

The respiration rate 70 BPM was not done with this measurement series, because all the measurements from section 4.1 and 4.2 are done with the respiration rate 70 BPM. The results of measurement 2 in shown in section 4.2 with angle φ = 180° and angle θ = 30°, θ = 50° and θ = 70° are added to figure 4.4. This can be seen in de Appendix in figure A.4. It can be seen that:

- the amplitude at θ = 70° is higher than the other respiration rates at θ = 70°;
- the number of pixels is at θ = 50° higher than the other respiration rates and at θ = 70° is much lower;
- the RMSE at θ = 50° have a large standard deviation. The other respiration rates have a constant RMSE at different angles and a small standard deviation.
- the SNR at θ = 30° is higher than the other respiration rates.

The measurements from section 4.2 differ from the measurements from section 4.3, this is because the position of the camera has not been the same. The angles were determined with a geo triangle and the distances were determined with a ruler. This can always deviate 2° and 3 cm, respectively.
Further, a non-equal part of the hot and cold pack is visible. This can be seen in the temperature images in the Appendix figure A.2 for the results of section 4.2 and figure A.3 for the results of section 4.3.
My conclusion of this measurement is that all the respiration rates can be detected, but it is difficult to perform measurements correctly.

4.4 Vary the Distance and the Amplitude from the Camera to the Setup

The distance was varied from 20 cm to 40 cm in steps of 10 cm. Each chosen distance was measured for different amplitudes: 1 mm, 3 mm, 7 mm with each a different respiration rate 72 BPM, 69 BPM, 66 BPM, respectively. The temperature images for amplitude 1 mm for distance 20 cm to 40 cm can be seen in figure 4.5. The other temperature images for the amplitudes of 3 mm and 7 mm can be seen in the Appendix in figure A.5. The results of the measurement for different distances and amplitudes can be seen in figure 4.6.
In figure 4.6A the maximum amplitude temperature change is plotted against the distances. The amplitudes 1 mm and 3 mm at a distance 30 cm are higher than all the other measurements. It was expected that the amplitude of 1 mm at distance 30 cm was higher than the other measurements, because the temperature of the hot and cold pack of that measurement was the highest. The reason why the amplitude of 7 mm at distance 30 cm is also higher than the other measurement is unclear.
Further, the number of pixels in figure 4.6B decreases by increasing the distance for all the amplitudes and it varies between 500 and 1800 pixels.
In figure 4.6C is shown that for all the measurement the RMSE is below 4 BPM.
Finally, the SNR in figure 4.6D is increasing by increasing the distance.
My conclusion of this measurement is that the respiration rate can be detected by all varied amplitudes and distances. However the number of pixels decreases and the SNR increases by increasing the distance.

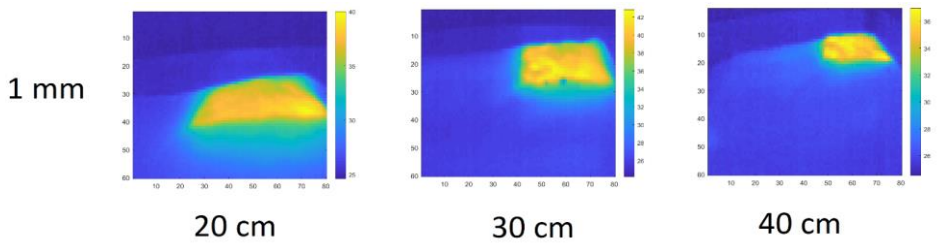

Figure 4.5: The temperature images for the amplitude of 1 mm can be seen for the setup with the distance varied from 20 cm to 40 cm, in steps of 10 cm. The other variables were fixed: angles φ = 90° and θ =70°.

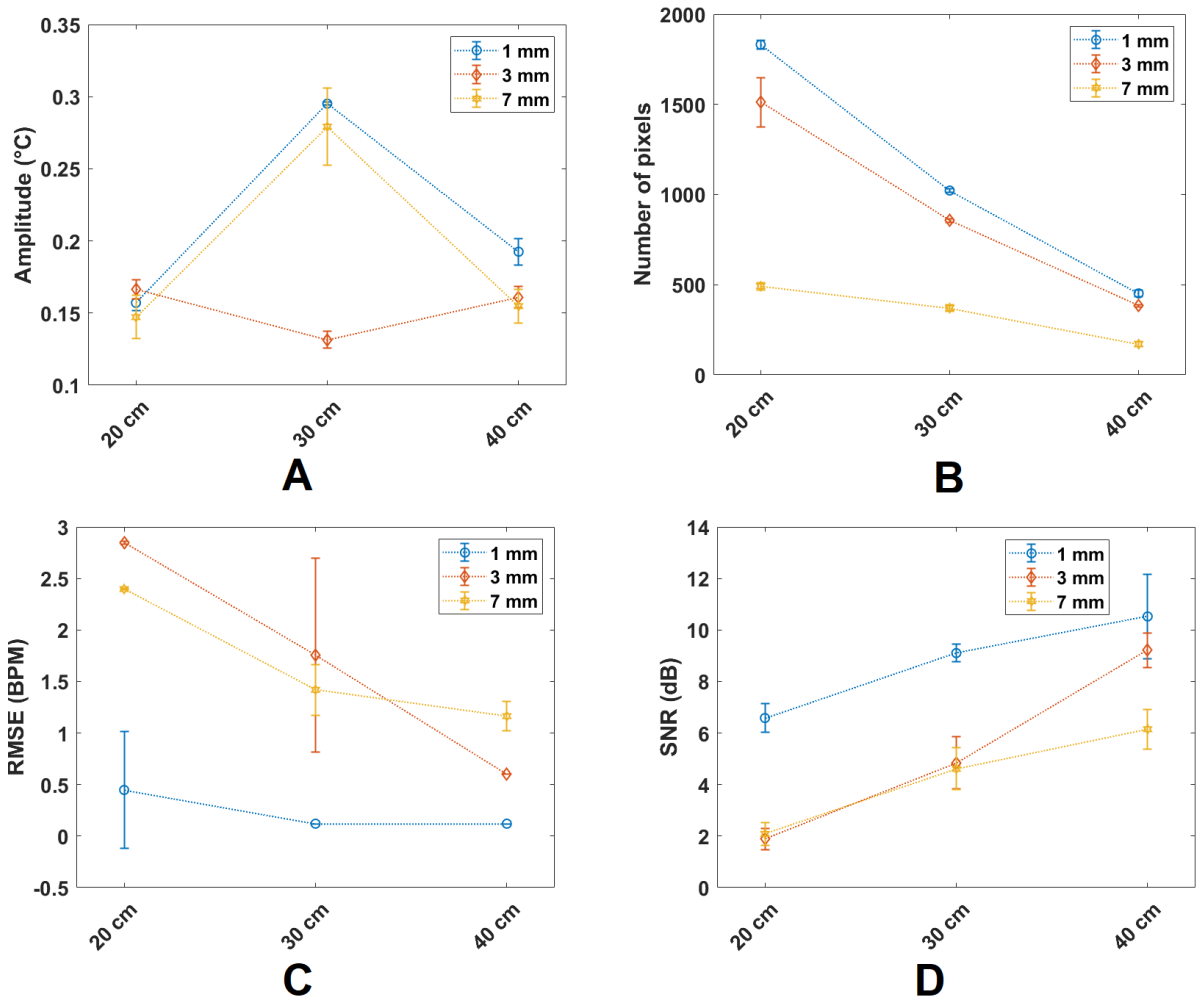

Figure 4.6: The results of measurement 4. The distance was varied from 20 cm – 40 cm. Each chosen distance were measured for different amplitudes: 7 mm, 3 mm, 1 mm with each an different respiration rate 67 BPM, 70 BPM, 73BPM, respectively. The other variables were fixed: angle θ = 70° and angle φ = 90°. Figure (A) shows the results of the amplitude in °C, figure (B) shows the number of pixels, figure (C) shows the RMSE in BPM and figure (D) shows the SNR in dB. The hot cold pack had a temperature between 36°C - 42°C.

5 Discussion

The goal is to build a test setup to measure simulated respiration rate due to the motion of the thorax.

5.1 Measurements

With the designed setup different parameters were varied to find out which position is the best for determining the respiration rate of the thorax. The respiration rate was detected for all varied parameters. For each measurement enough pixels were involved in detecting respiration and the variation in the detected frequency was low. Varying angle φ and θ showed that the best results are at φ = 120° to 180° and θ = 10° to 30°, then the SNR is the highest, the maximum amplitude change of the temperature is sufficient and the number of pixels is enough for detecting respiration rate. A schematic representation of the angles can be seen in figure 5.1.

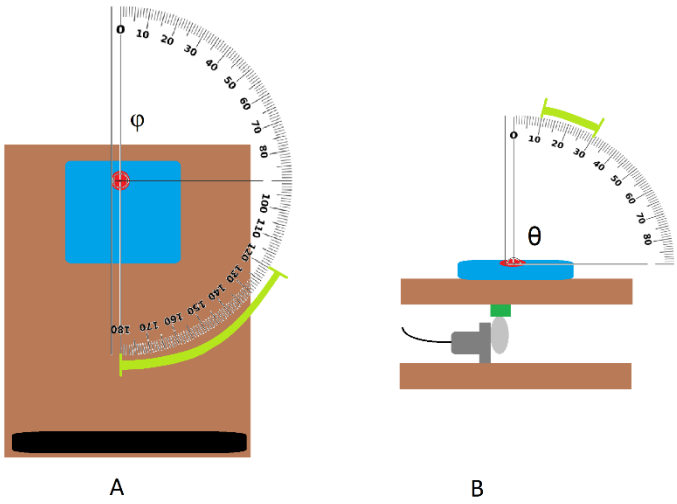

Figure 5.1: picture (A) shows the top view of the simulator showing how the angle φ was defined and picture (B) shows the front view of the simulator showing how the angle θ was defined. In both images the best angles are indicated with light green.

The third parameter that was varied was the respiration rate. The respiration rate was set at 42 BPM, 50 BPM, 61 BPM and 80 BPM at θ = 30°, θ = 50° and θ = 70°. The results showed for all the respiration rates that the number of pixels involved in respiration were enough to measure respiration, the maximum amplitude change of the temperature were sufficient and the standard deviation of respiration frequency was low. The SNR was high for respiration rate 61 BPM. The reason why the SNR was higher for the respiration 61 BPM was unclear. Further the results from the measurements done in section 4.2 differ from the measurements done in section 4.3. One of the main limitations of this setup is that re-performing measurements has a lot of influence on the results. The angles were determined with a geo triangle and the distances were determined with a ruler. This can deviate 2° and 3 cm, respectively. In short, the respiration rate has no influences and re-performing measurements has a lot of influences on the measurements.

The fourth and fifth parameter that were varied were the amplitude and the distance. The amplitudes were set at 1 mm, 3 mm and 7 mm, and the distance was set at 20 cm, 30 cm and 40 cm. The results showed for all the distances and amplitudes that maximum amplitude change of the temperature was sufficient and the standard deviation of respiration frequency was low. As expected, the number of pixels decreases, for all the amplitudes, by increasing the distance. But which was not expected was that the SNR increased, for all the amplitudes, by increasing the distance. In short, the amplitude has no influences on the measurements. However the number of pixels involved in respiration rate decreases and the SNR increases by increasing the distance.

The general problem was the temperature of the heat source. The results from the test setup showed that the warm water bag was not suitable for the setup, so the warm water bag was replaced by a hot and cold pack, because the hot and cold pack gave a better heat distribution. The temperature of the hot and cold pack was not constant, and this had influence on the maximum amplitude change of the temperature. The amount of hot and cold pack that comes into the thermal camera view also had influences the results.
So, the conclusion is that the optimal position is at angle φ = 120° to 180° and angle θ = 10° to 30° and that the setup and the measurements have some limitations.

5.2 Limitations

There are limitations in this work with respect to the developed simulator and the measurements. First the limitations of the developed simulator are discussed.
The first limitation was the heat source. First a warm water bag was used, but this was not homogeneous. This was due to the thick edges of the warm water bag, so that it was not heated properly by the warm water. The warm water bag was replaced by a hot and cold pack. This gave a better homogeneous heat distribution. The hot and cold pack had a square shape, which was clearly visible with the thermal camera. In addition, the temperature of the hot and cold pack was not constant. It varied between 36°C - 42°C. This is because the hot and cold pack needed to be reheated a several times.
The second limitation was de size of the setup. The setup was placed on an infant bed. The height difference between the lower wooden board and the wooden board that moves up and down was 14 cm. The heat source that needs to mimic the infant was put on the upper wooden board. But due to this height difference between the top board and the bed, the bottom of the heat source and its movement was also measured. The movement of the bottom moves in the opposite phase as the top part of the heat source.
The third limitation was the movement of the setup. Real life breathing is not only an up and down movement but likely a more complex pattern. In addition, at the end of the top board the amplitude was 7 mm and at the end of the top board the amplitude was 1 mm. This amplitude was determined from the center of the hot and cold pack. So, one side of the hot and cold pack has a larger amplitude than the other side of the hot and cold pack. In short, the amplitude was not constant across the hot and cold pack. Further, the possible shoulder movement of the infant was not considered.
The fourth limitation was the speed controller. The speed controller of the setup was continuous, and it did not have an easy rotary knob, but with a screwdriver a small screw had to be turned to change the speed. As a result, a specific frequency cannot be set or found back easily. Furthermore, the speed of the engine also depends on the weight that was placed on the top shelf.
There are also limitations with the measurements. The first limitation was the consistency of the measurements. Re-performing measurements has a lot of influence on the results. The angles were determined with a geo triangle and the distances were determined with a ruler. Thus, the positioning accuracy was low.
The second limitation was the amount of hot and cold pack that comes into the thermal camera view, because this influences the number of pixels and the SNR.
The third limitation was the temperature of the heat source, because this influence the maximum amplitude change of the temperature.

6 Conclusions and Recommendations for Further Research

In this study, a setup to simulate the respiratory motion of a neonatal chest was designed and measurements at different settings and positions in order to determine the best camera position were performed. The setup works and can simulate breathing though there are limitations as it deviates from real neonatal breathing, mainly because the amplitude used is large for a neonate, and the temperature was not constant and mainly higher than the body temperature of an infant. The respiration rate was determined for all different angles φ and θ, respiration rate, distances and amplitudes.

From the position testing, it was determined that the best vertical angle φ is between 120° to 180°, and the best horizontal angle θ is between 10° to 30°. Moreover, the higher the temperature of the heat source, the higher the maximum amplitude change of the temperature. Furthermore, different respiration rates and amplitudes had no influences on determining the respiration rate. Besides, the number of pixels decreases by increasing the distance. In addition, re-performing measurements has a lot of influences on the measurements.

There are several limitations to the designed setup and if further research is to be done with this setup several things have to be changed. In the used setup a hot and cold pack with a square shape was used for the heat source. For further research, a homogeneous heat source in the shape of an infant must be used. The other body parts must also be considered. This could affect the results of the position of the thermal camera. Also, the temperature needs to be constant. A heat source that is constantly monitoring the temperature can be considered. Furthermore, the height difference between board that moves up and down and the bed must be 0 cm. This can be solved, for example, by placing the setup in the mattress or by building something around it that has the same height as the top board. Moreover, the up and down movement of the setup needs to be improved, because the amplitude depends on the position of the heat source on the top board. Also, the shoulder movement must be considered. Furthermore, the speed controller must be calibrated and made more user-friendly. Finally, a better way must be found to determine the distance and angles of the thermal camera to ensure that the camera is in the same position.

Reference

[1] Honings, I. (2019). Measuring respiration rate in settings with a thermal camera. Technical University Eindhoven.

[2] K. Abbas, K. Heiman, T. Orlikowsky, S. Leonhardt. (2009). Non-contact Respiratory Monitoring based on Real-time IR-Thermography. In world Congress on Medical Physics and BioMedical Engineering. Munich. Germany. Springer. Berlin. Heidelberg. P.1306-1309.

[3] G. Yuan, N.A. Drost, R.A. McIvor. (2013). Respiratory Rate and Breathing Pattern. McMaster University Medical Journal 10,1. 23-25.

[4] C.B. Pereira, X. Yu, M. Czaplik, V. Blazek, B. Venema, S. Leonhardt. (2016). Estimation of breathing rate in thermal imaging videos: a pilot study of healty human subjects. Journal of clinical monitoring and computing. 31.

[5] C.B. Pereira, X. Yu, M. Czaplik, R. Rossaint, V. Blazek, S. Leonhardt. (2015). Remote monitoring of breathing dynamics using infrared thermography. Biomedical Optics Express. 6. 4378.

[6] Maxima Medisch Centrum (MMC) in Veldhoven, the netherlands, Photoarchive

[7] Dimitriou, G., Greenough, A., & Laubscher, B. (1996). Lung volume measurements immediately after extubation by prediction of "extubation failure" in premature infants. Pediatric pulmonology. 21, 4. 250-4 .

[8] K. Abbas, K. Heimann, K. Jergus, T orlikowsky, S. Leonhardt. (2011). Neonatal non-contact respiratory monitoring based on real-time infrared thermography. BioMedical Engineering On-Line. 10. 93.

[9] M. van Scherpenzeel. Alles over vroeggeboorte baby. Ouders van nu. Retrieved August 28, 2019, from https://www.oudersvannu.nl/zwanger/complicaties/vroeggeboorte/.

[10] P. Orbanz, J. Buhmann. (2008). Nonparametric Bayesian image segmentation. International Journal of Computer vision 77. 1-3: 25-45.

[11] C. Bird, (2019, June 20). All About the Neonatal Intensive Care Unit (NICU). Verywell family. Retrieved August 28, 2019, from https://www.verywellfamily.com/all-about-the-nicu-2748422.

[12] 'Premature and Newborn size chart'. Touching Little lives. Retrieved September 24, 2019, from https://www.touchinglittlelives.org/size.html.

[13] C.B. Pereira, X. Yu, T. Goos, I. Reiss, T. Orlikowisky. (2018). Noncontact monitoring of Respiratory Rate in Newborn Infants Using Thermal Imaging. IEEE Transactions on BioMedical Engineering. 66(4), 1105-1114.

[14] J.M. Di Fiore. (2004). Neonatal cardiorespiratory monitoring techniques. Seminars in neonatology. Vol. 9. No. 3. 195-203.

[15] I. Lorato, T. Bakkes, S. Stuijk, M. Meftah, G. de Haan. (2019). Unobtrusive Respiratory Flow Monitoring Using a Thermopile Array: A Feasibility Study. Applied sciences 9.12: 2449.

[16] A.S. Scavacini, M.H. Miyoshi, B.I. Kopelman, C. Areaújo peres. (2007). Chest expansion for assessing tidal volume in premature newborn infants on ventilators. Jornal de pediatria. 83.4: 329-334.

[17] M. Nano. (2015). Automated Detection of Central Apnea in Preterm Infants.

[18] R. Martin, 'Chapter 157: Pathophysiology of Apnea of Prematurity'. Pathophysiology of Neonatal Diseases. 1595 – 1603.

[19] Couveuse ouders. Couvese. Couvese ouders, Retrieved September 9, 2019, from https://www.couveuseouders.nl/neonatologie/apparatuur/couveuse/.

[20] M. Villarroel, A. Guazzi, J. Jorge, S. Davis, P. Watkinson. (2014). Continuous non-contact vital sign monitoring in neonatal intensive care unit'. Healthcare technology letters. 1(3). 87-911.

[21] J. Jorge, M. Villarroel, S. Chaichulee, A. Guazzi, S. Davis. (2017). Non-contact monitoring of respiration in the neonatal intensive care unit. IEEE International Conference on Automatic Face & Gesture Recognition (FG 2017). 286-293.

[22] Majo Clinic. Premature birth: Symptoms & Causes. Retrieved September 13,2019, from https://www.mayoclinic.org/diseases-conditions/premature-birth/symptoms-causes/syc-20376730

Appendix

The temperature images from the results of section 4.2 can be seen for the setup with the hot and cold pack with the angle θ varied from 0° to 70°, with steps of 10°. This measurement was done for a fixed φ = 90° and φ = 180°.

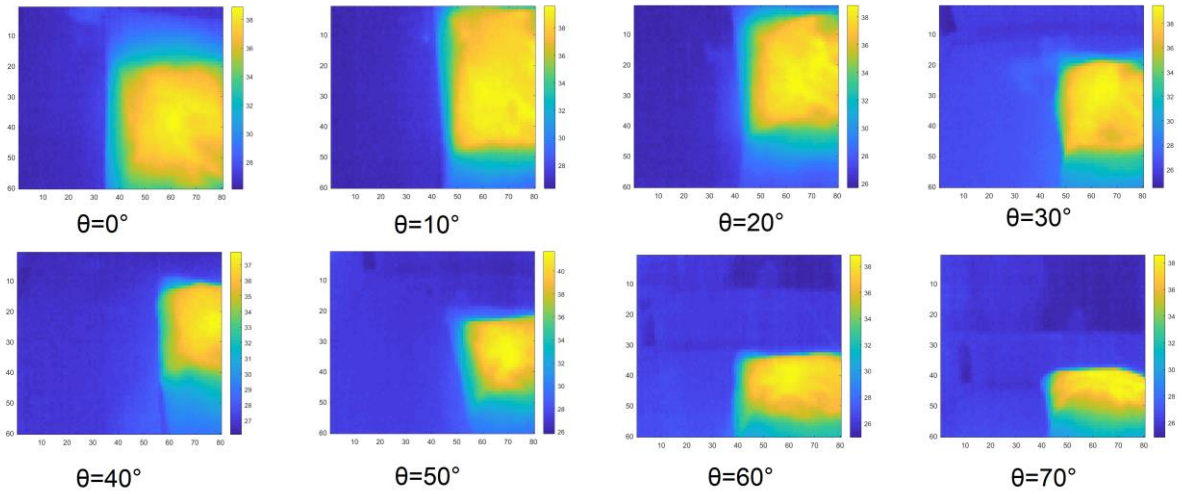

Figure A.1: The temperature images for θ varied from 0° to 70°, with steps of 10°. The hot cold pack had a temperature between 37°C - 41°C. The other variables were fixed: φ = 90°, the respirate rate was 70 BPM, the distance was 20 cm and the amplitude was 7 mm.

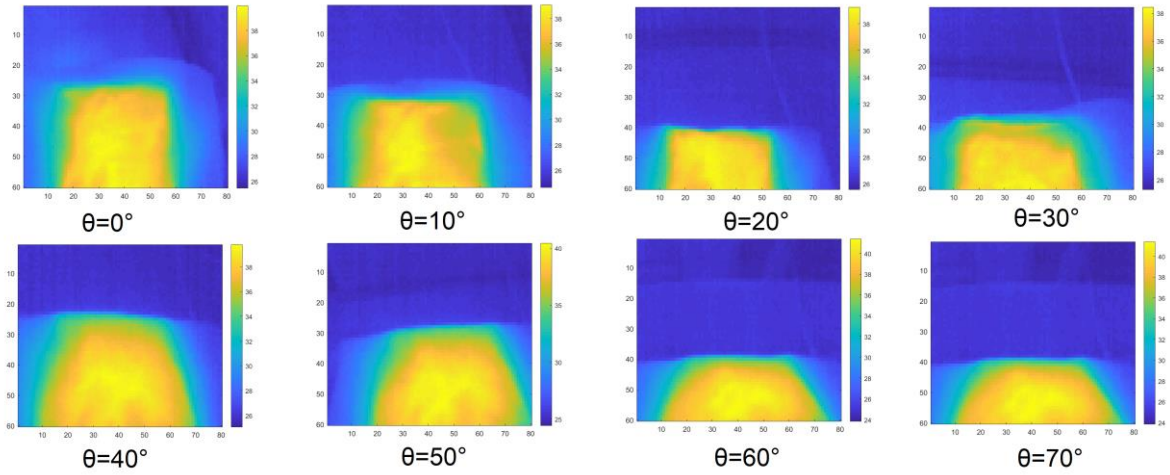

Figure A.2: The temperature images for θ varied from 0° to 70°, with steps of 10°. The hot cold pack had a temperature between 38°C - 41°C. The other variables were fixed: φ = 180°, the respirate rate was 70 BPM, the distance was 20 cm and the amplitude was 7 mm.

The temperature images from the results of section 4.3 of the respiration rates: 42 BPM, 50 BPM, 61 BPM and 80 BPM can be seen for the setup with the angle θ = 30°, 50° and 70°. This measurement was done for a fixed φ = 180°.

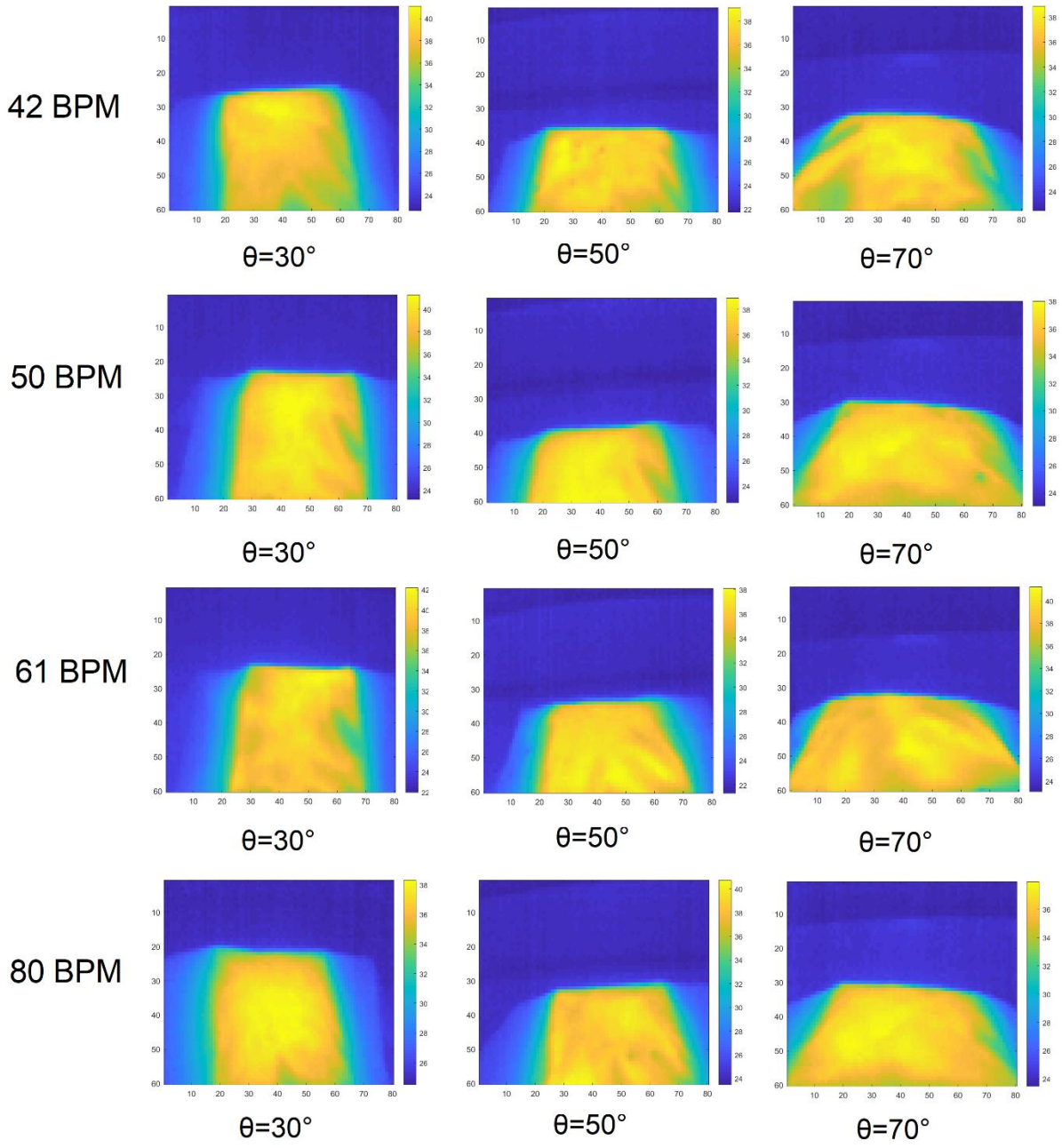

Figure A.3: The temperature images for the respiration rate 42 BPM, 50 BPM, 61 BPM and 80 BPM can be seen for the setup with the angle θ = 30°, 50° and 70°. The hot cold pack had a temperature between 36°C - 42°C. The other variables were fixed: φ = 180°, the distance was 20 cm and the amplitude was 7 mm.

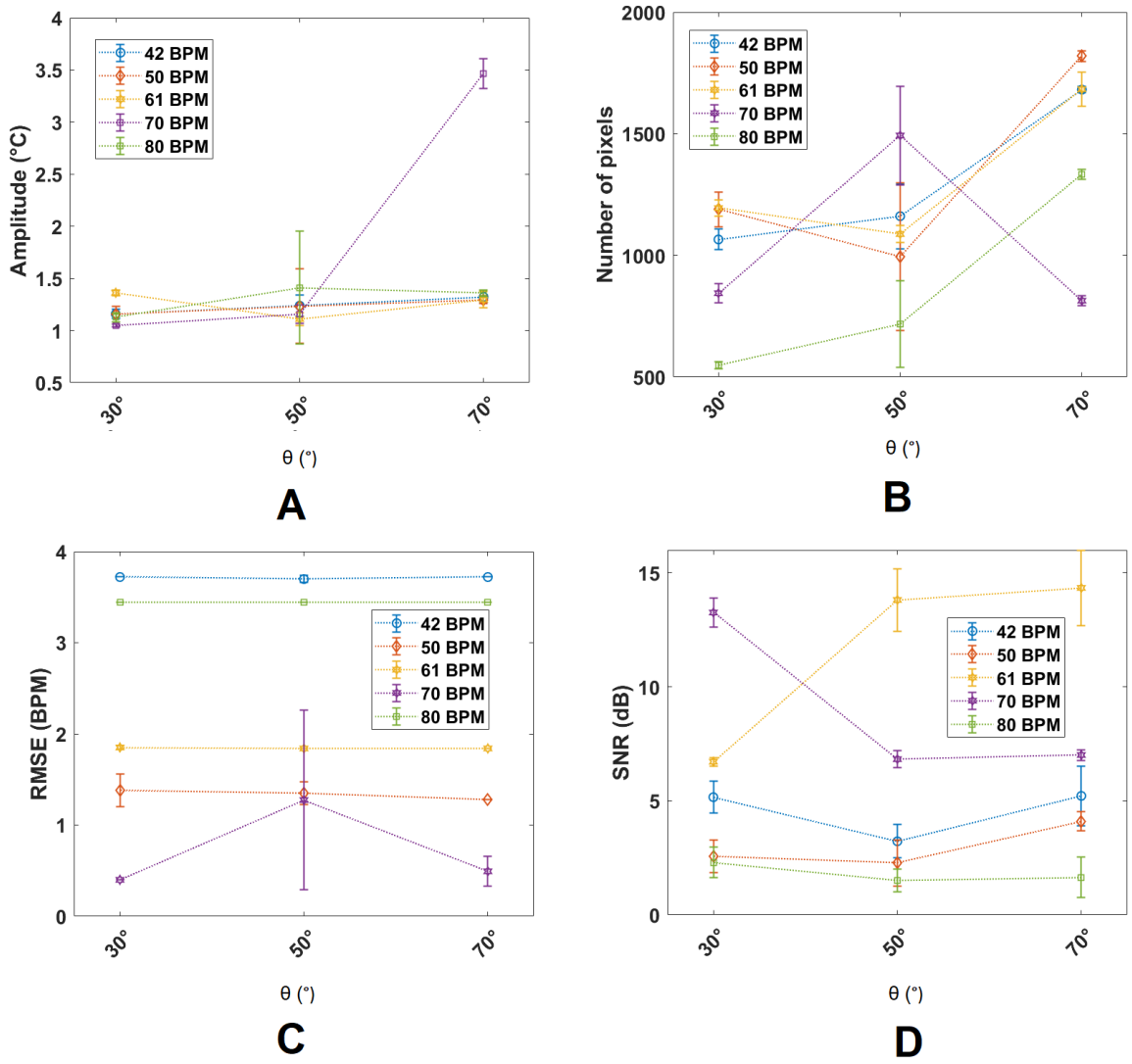

Figure A.4: The results of measurement 3 + respiration rate 70 BPM from measurement 2 are plotted. For the angles: θ = 30°, 50° and 70° the respirate rates were: 42 BPM, 50 BPM, 61 BPM, 70 BPM and 80 BPM. The other variables were fixed: φ = 180°, the distance was 20 cm and the amplitude was 7 mm. Figure (A) shows the results of the amplitude in °C, figure (B) shows the number of pixels, figure (C) shows the RMSE in BPM and figure (D) shows the SNR in dB. The hot cold pack had a temperature between 36°C - 42°C.

The temperature images from the results of section 4.4 of the amplitudes: 1 mm, 3 mm and 7 mm can be seen for the setup with the distance varied 20 cm, 30 cm and 40 cm. This measurement was done for a fixed angles φ = 90° and θ= 70°

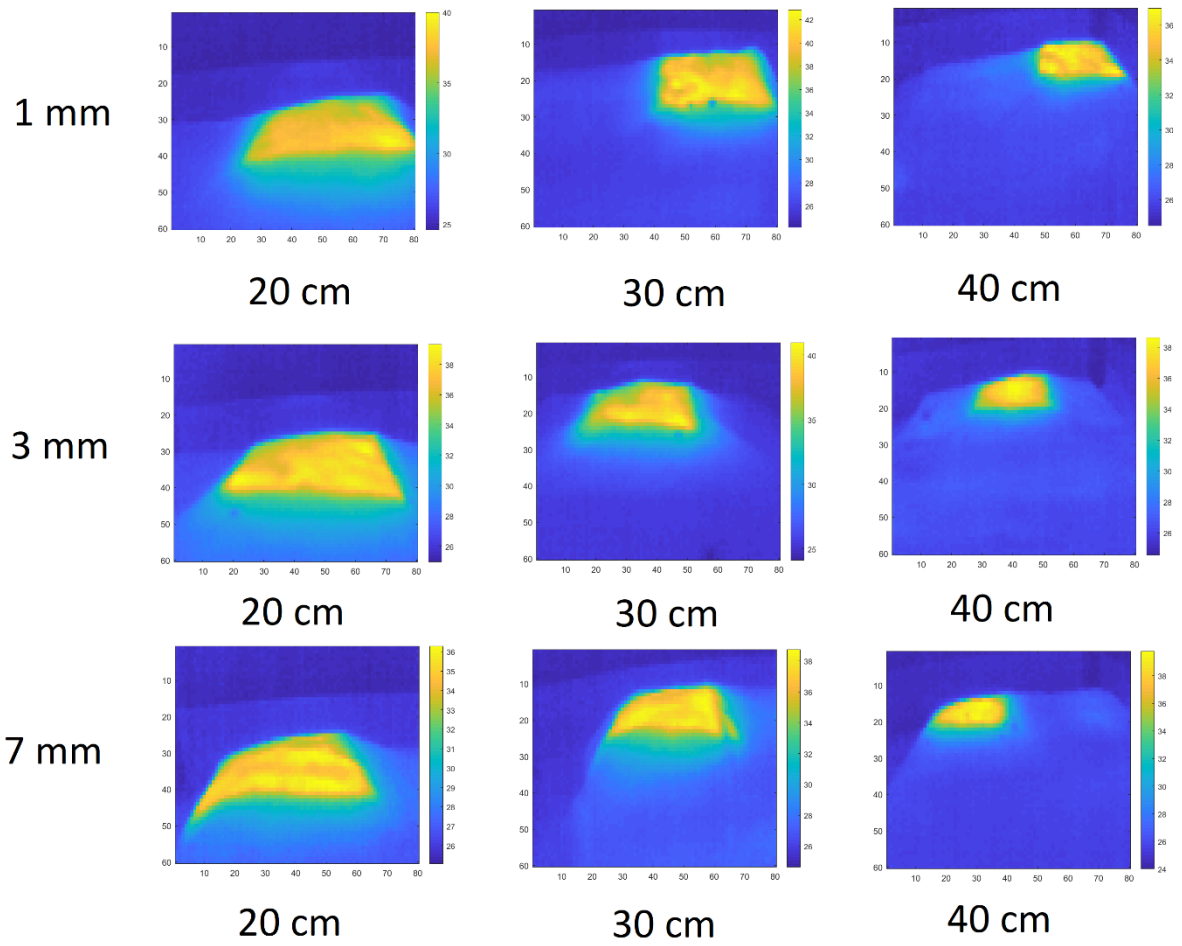

Figure A.5: The temperature images for the amplitudes: 1 mm, 3 mm and 7 mm can be seen for the setup with the distance varied from 20 cm to 40 cm, in steps of 10 cm. The other variables were fixed: angles φ = 90° and θ =70°.